The
ENGINEERS' DIGEST

REVIEW OF ENGINEERING PROGRESS ABROAD

VOL. VI. No. 7

ENGINEERING LIBRARY

SEP 7 1945

JULY, 1945

Churchill
PRECISION GRINDING MACHINES
GRINDING FROM THE SOLID ECCENTRIC FINS ON AERO ENGINE CYLINDERS USING A MULTI-RIBBED WHEEL
There is a CHURCHILL machine for every precision grinding job..
THE CHURCHILL MACHINE TOOL CO., LTD., MANCHESTER.
HOME SELLING AGENTS . . . . . CHARLES CHURCHILL & CO. LTD. (BIRMINGHAM & BRANCHES)
EXPORT SALES ORGANISATION . . ASSOCIATED BRITISH MACHINE TOOL MAKERS Ltd. (London & Branches)

THE ENGINEERS' DIGEST

REVIEW OF ENGINEERING PROGRESS ABROAD

Published Monthly at 120, Wigmore Street, London, W. 1.

Publishers : **ENGINEERS' DIGEST LTD.** – – – – – – Telephone : WELBECK 9357

Advertisement Dept. – 120, Wigmore Street, London, W.1. – – Telephone : WELBECK 9357

Distribution – – E. & F. N. SPON, LTD., 57, Haymarket, London, S.W.1.
Telephone : Whitehall 1860. Telegrams : Fenspon, Lesquare, London

Editorial Dept. – – 120, Wigmore Street, London, W.1. – – Telephone : WELBECK 9357

Subscriptions to : ENGINEERS' DIGEST LTD., 120, Wigmore Street, London, W.1, or
E. & F. N. SPON, LTD., 57, Haymarket, London, S.W.1.

ANNUAL SUBSCRIPTION OF 12 NUMBERS, £2 2s. **SINGLE COPIES, 4s. 6d.**

ADVISORY COMMITTEE

J. F. ALCOCK, B.A., A.M.I.Mech.E.
R. W. ALLOTT, M.A., A.R.Ae.S.
E. ALTON, D.Eng., A.M.Inst.B.E.
H. H. ASBRIDGE, M.B.E., M.I.Mech.E.
R. W. AYERS, M.I.W.
Col. J. BOWDEN, M.Inst.C.E., M.I.Mech.E.
H. H. BROUGHTON, M.I.Mech.E.
F. BUCKINGHAM, B.Sc., A.M.Inst.C.E., A.M.I.Mech.E.
T. H. BURNHAM, B.Sc. (Lond.), A.M.I.Mech.E. [A.M.I.E.E.
J. S. CASWELL, M.Sc., M.I.Mech.E.
G. C. SAFFERY COOPER.
J. DICK, Ph.D., B.Sc., A.M.I.Mech.E.
D. FIFE, M.I.Mech.E.
G. E. FOXWELL, D.Sc. (Lond.), F.Inst.P., F.Inst.F.,
R. GRIFFITHS, M.Sc. [M.Inst.Gas.E.
H. HEYWOOD, Ph.D., M.Sc. (Eng.), A.M.I.Mech.E.
O. HURST, M.Inst.N.A.
Capt. J. S. IRVING, M.I.Mech.E., M.I.A.E., A.F.R.Ae.S., M.S.A.E.
F. C. JOHANSEN, M.Sc. (Eng.), M.I.Mech.E., F.R.Ae.S., M.I.Loco.E.
W. J. KEARTON, D.Eng., M.I.Mech.E., A.M.Inst.N.A.
Prof. W. KERR, Ph.D., M.I.Mech.E.
G. V. LOMONOSOFF, Dr.Ing., M.I.Mech.E.
B. J. LYMER, M.I.Mech.E.
D. T. MacIVOR, M.I.Mech.E., M.Cons.E.
W. O. MANNING, F.R.Ae.S.
R. B. MATTHEWS, Wh.Ex., A.M.Inst.C.E., M.I.E.E., F.R.Ae.S.
Prof. A. L. MELLANBY, D.Sc., LL.D., M.I.Mech.E.
J. H. R. RATCLIFFE, B.Sc. (Eng., Hons.), M.I.Mech.E.
Col. C. W. D. ROWE.
W. A. SCOBLE, D.Sc., A.R.C.Sc., M.I.Mech.E.
P. W. SEEWER, D.E. (Zurich), M.Inst.C.E., M.I.Mech.E.
Prof. S. PARKER SMITH, D.Sc., M.I.E.E., A.M.Inst.C.E.
C. F. H. VERITY, A.M.Inst.C.E., A.M.I.E.E., A.M.I.Mech.E.
E. G. WALKER, F.C.G.I., B.Sc. (Eng.), M.Inst.C.E., M.I.Mech.E., M.Am.Soc.C.E.
Major F. L. WATSON, M.Inst.C.E., M.I.Mech.E.
G. WATSON, M.Inst.C.E., M.I.Mech.E.
C. H. WOODFIELD, M.I.Mech.E., M.I.Struct.E.
T. WRIGHT, Ph.D., M.Sc.
M. L. YATES, Ph.D., M.Sc.Tech., M.A. (Com.), M.I.Mech.E.

"Cronite"
REGD. TRADE MARK
The HIGH TEMPERATURE ALLOY
SALT, LEAD AND CYANIDE VESSELS
CARBURIZING BOXES AND POTS
ROTARY RETORTS & PROPELLING WORMS
FURNACE HEARTHS AND FITTINGS
ENAMELLING PERRITS AND SUPPORTS
GLASS-BLOWING NOZZLES
PYROMETER PROTECTION SHEATHS
CASTINGS FOR USE AT 700°/1200° C.
The CRONITE FOUNDRY Co. LTD
LAWRENCE RD · TOTTENHAM · LONDON N15
PHONE · STAMFORD HILL 4237

CONTENTS

page

Age Hardening of the Solid Solution Aluminium-Zinc 183
"*The Engineers' Digest*," *Vol.* 6, *No.* 7, *p.* 183.

Carbon, a Material for Switch and Control Gear 185
"*The Engineers' Digest*," *Vol.* 6, *No.* 7, *p.* 185.

Ceramic Insulating Materials at High Temperatures 174
"*The Engineers' Digest*," *Vol.* 6, *No.* 7, *p.* 174.

Direct Resistance Heating of Salt Baths for the Patenting of Steel Wire 169
"*The Engineers' Digest*," *Vol.* 6, *No.* 7, *p.* 169.

Instruments for Technical Stroboscopy 187
"*The Engineers' Digest*," *Vol.* 6, *No.* 7, *p.* 187.

Measurements of Small Motions 192
"*The Engineers' Digest*," *Vol.* 6, *No.* 7, *p.* 192.

On Flywheel Design 170
"*The Engineers' Digest*," *Vol.* 6, *No.* 7, *p.* 170.

Radial and Lateral Reactions acting upon the Wheels of a Motor Car 175
"*The Engineers' Digest*," *Vol.* 6, *No.* 7, *p.* 175.

The Brittleness of the Enamel of Coated Aluminium Wire at Normal and Higher Temperatures .. 190
"*The Engineers' Digest*," *Vol.* 6, *No.* 7, *p.* 190.

Thermal Stresses in Discs 172
"*The Engineers' Digest*," *Vol.* 6, *No.* 7, *p.* 172.

Introducing

MIRROFLECT WELDING GLASS

A NEW ACTARC PRODUCT

At last a long felt want is supplied by Actarc, the "Mirroflect" has passed National Physical Laboratory Tests and conforms to B.S.S. 679.

It is so designed that you are able to see not only the part to be welded, but all around it. Actarc Mirroflect enables your welders to see the job correctly and consequently increases output.

Actarc Mirroflect is laminated—thus reducing risk of breakage. Will not let harmful rays pass and affect your operators' eyes. Ask your operators' opinions on this remarkable innovation.

Made in two sizes: $4\frac{1}{4} \times 3\frac{1}{4}$, $4\frac{1}{4} \times 2\frac{1}{8}$; and three grades: C (Light), D (Medium), E (Dark).

ACTARC SUREARC

ARC MANUFACTURING CO., LTD.

PROPRIETORS OF THE SURE-ARC ELECTRODE CO., LTD.

ACTARC WORKS, GOLDHAWK ROAD, LONDON W.12

REGD. TRADE MARK

TELEPHONE: SHE 1151 TELEGRAMS: ACTIVARC, PHONE, LONDON. CABLES: ACTIVARC, LONDON.

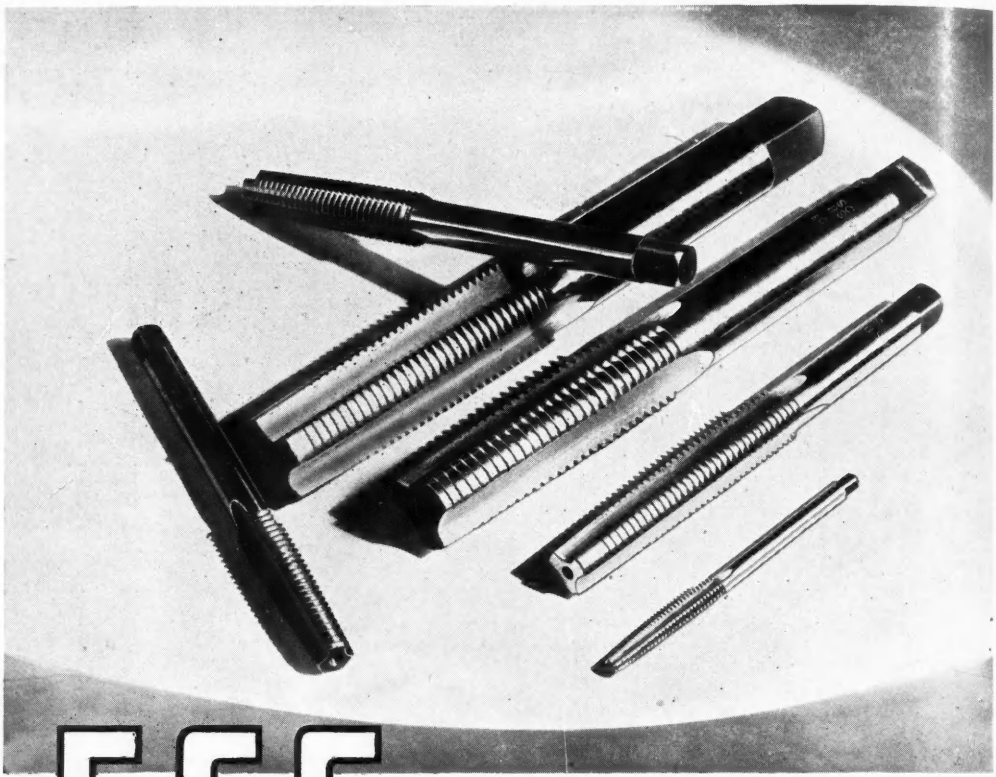

ESC GROUND THREAD TAPS

Conform to the provisions of British Standard Specifications 949/1941.

With our modern plant and equipment, we make Ground Thread Taps, Chasers, etc., of an accuracy of pitch and refinement of form unobtainable with cut form thread tools. Complete Range of Ground Thread Taps in production, most of which can be delivered from Stock.

ENGLISH STEEL CORPORATION LTD

OPENSHAW MANCHESTER

DIRECT RESISTANCE HEATING OF SALT BATHS FOR THE PATENTING OF STEEL WIRE.

By W. HEIDENHAIN. (From *Stahl & Eisen*, Vol. 64, 1944, pp. 747-751).

INVESTIGATIONS into the resistance heating of salt baths used in the patenting of steel wire have led to the development of a method in which the molten salt contents of the pot act as the resistor. In cases where the distance between the plate electrodes is large the heating process is initiated by creating a liquid bridge between the electrodes by means of a special electric heating ribbon extending between the electrodes. This ribbon is removed from the bath after the flow of current between the electrodes has been established.

A diagrammatic view of the bath installation is given in Fig. 1, which shows the pot (*a*) in section with the electrodes (*b*) being installed at two opposite sides of the pot. The dimensions of the electrodes are chosen in accordance with the width of the pot and its cubical contents. A single phase transformer (*c*) of special design is installed in the immediate vicinity of the bath in order to keep the electrode leads as short as possible, thus minimising electric loss in the leads. In order to eliminate the conduction of heat from the electrodes to the transformer, and also to prevent the radiation of heat from the bath to the leads, the latter are water cooled. The electric current passing through the bath is automatically controlled. The control circuit comprises the thermostat (*f*), the chopper-bar type instrument (*k*), and the relay operated switch (*i*).

The pot (*a*) is well insulated by a thick layer of infusorial insulating material (Sterchamol) in order to minimise radiation loss. The electric circuit of the

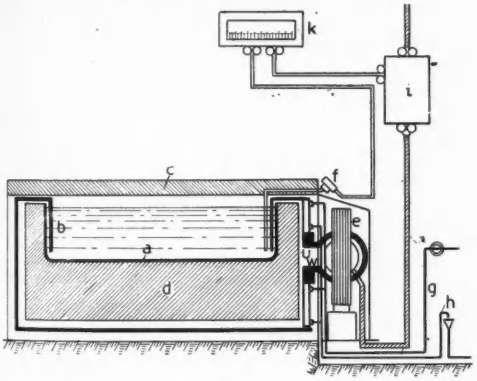

Fig. 1.

installation is shown in Fig. 2. The current required for heating the bath is taken from two phases of a three-phase network of 380/220 volts, the primary of the transformer having a tap switch *S*. The main switch (*i*) is actuated by an auxiliary relay (i_1) which closes a circuit between the phase *T* and the neutral *O*. The auxiliary relay is actuated by the thermo-couple (*f*) and the aforementioned indicating instrument (*k*). The output of the single-phase secondary of the transformer, which depends upon the current passing between the electrodes, can be controlled by means of the tap-switch (*s*) of the primary.

The heating plant is operated as follows: Operation is started by connecting the bath electrodes by a steel tape acting as resistor. As soon as this resistor has supplied sufficient heat to the solid salt contents of the bath to form a liquid bridge between the electrodes, the heating current will begin to flow between the latter, and the steel tape may then be removed from the bath.

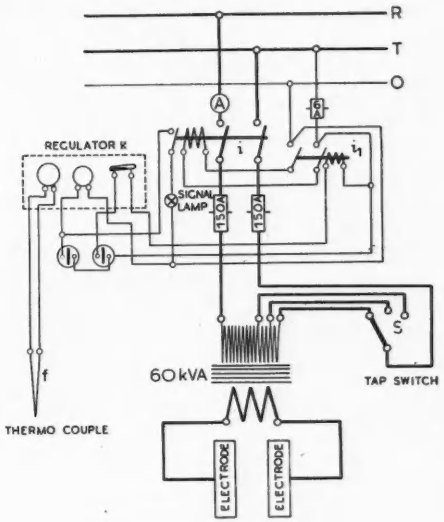

Fig. 2.

In order to speed up the process of starting the bath, increased voltage is supplied until the bath has come up to temperature. The voltage is then gradually decreased in order to keep the transformer load from rising above its rated value of 60 KVA. The load taken by the steel tape is 50 KVA and the initial load of the electrode circuit is 35 KVA. This load decreases to 17 KVA upon the attainment of normal operating conditions.

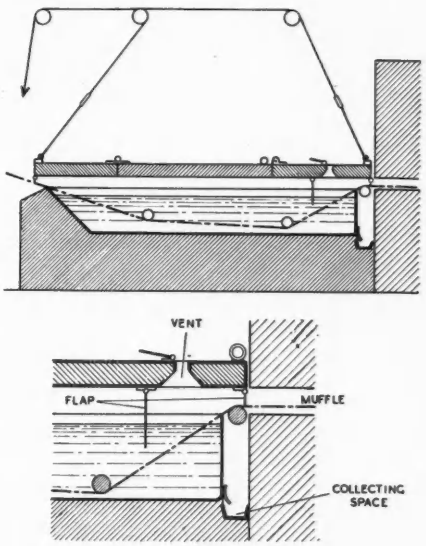

Fig. 3.

After the entire contents of the bath have become liquid, the tap switch is moved to the lowest tap. This point corresponds to the heat supply required under normal operating conditions when a certain amount of heat is transmitted to the bath from the steel wire as it passes through the bath. This ensures a minimum current density in the bath, minimum electrolytic effect, and minimum evaporation of salt during the short heating periods. According to operating records, the electric power consumption amounts to 35 KW hr. per ton of 1.8-3.6 mm. dia. wire passed through the bath. This is only one-fifth to one-sixth of the power consumption required with the employment of a ribbon-type resistor.

The cover of the pot is carefully designed to ensure removal of the salt vapours at the source. Referring to Fig. 3, it is seen that the cover is hinged at the side of the pot adjoining the muffle. The cover is thus lifted in the direction of the travel of the wires through the bath, its front end resting lightly upon the wires where they leave the bath. This design prevents salt vapours from seeping into the muffle furnace. As Fig. 3 also shows, a pendulous flap is attached to the underside of the cover at a certain distance from the point at which the wires enter the bath. In this way only a very small portion of the surface of the bath is in communication with the delivery opening of the muffle furnace, while the vapours escaping from this part of the bath surface are vented through one or several openings provided in the cover.

The accumulation of sludge at the bottom of the bath is kept to a minimum owing to the thorough sealing of the muffle furnace, and it amounts to no more than 300 kg. per week. The presence of these deposits is without influence upon the heat transfer, and the efficiency of the heating device is not therefore effected. Nor can local overheating take place.

Owing to the tendency of the salt to creep over the rim of the pot, both salt and scale were found to accumulate in the clear space between pot and furnace at the point where the wires enter the bath. In order to facilitate the removal of these deposits, a deflector plate was attached to the side of the pot, as indicated in Fig. 3.

This type of direct resistance heating has proven its value in nine months of continuous service.

ON FLYWHEEL DESIGN.

By I. I. ARTOBOLEVSKY. (From *Comptes Rendus (Doklady) de l'Académie des Sciences de l'URSS*, 1944, Soviet Academy of Sciences, Vol. 44, No. 5, pp. 182-185).

IN modern engineering practice the required flywheel inertia in a machine is usually found by the method of excess moment diagrams which was suggested by Radinger(1). Another generally used method consists in plotting kinetic energy—reduced mass diagrams—according to Wittenbauer(2). 'Radinger's method is very simple, but it gives only an approximate solution, and its application is confined to the design of machines whose motion is characterised by low coefficients of unsteadiness; Wittenbauer's method is free from the assumptions made by Radinger, but it suffers from the disadvantage that it entails the necessity to plot a number of intermediate functions, which generally leads to considerable errors in the ultimate results. A solution similar to Wittenbauer's method has been proposed by Merzalov(3) and Gutjar(4).

It is the purpose of the present investigation to show that the method of excess moment diagrams can give a rigorous solution of the problem without resorting to the assumptions made by Radinger. The use of this method does not therefore depend upon whether the run of the machinery is characterised by a low or a high co-efficient of unsteadiness.

As is well known (5), the equation of motion of a mechanism can be written in the general form as follows

$$M_d - M_r = I_r \frac{d\omega}{dt} + \frac{d I_r}{d\varphi} \frac{\omega^2}{2} \quad .. \quad (1)$$

where M_d is moment of reduced driving force; M_r is moment of reduced resistance force; I_r is reduced moment of inertia of the mechanism; ω is angular velocity of the reduction link.

The reduced mass I_r of the mechanism can always be represented thus

$$I_r = I_o + \Delta I_r \quad .. \quad .. \quad (2)$$

where I_o is the constant moment of inertia of the flywheel which must be determined; and ΔI_r is the reduced mass of all the remaining links of the mechanism. Denoting the difference $M_d - M_r$ by ΔM, equation (1) can now be rewritten in the following form

$$\Delta M = (I_o + \Delta I_r) \frac{d\omega}{dt} + \frac{d(\Delta I_r)}{d\varphi} \frac{\omega^2}{2} \quad .. \quad (3)$$

Let us consider the positions of the mechanism in which the angular acceleration of its driving link is zero, that is, $\frac{d\omega}{dt} = 0$. Clearly, in these positions the angular velocity is either at maximum, ω_{max}, or at minimum, ω_{min}. Accordingly, equations (3) for these positions will take the form

$$\Delta M' = \frac{d(\Delta I_r)}{d\varphi} \frac{\omega^2_{max}}{2} \quad .. \quad .. \quad (4)$$

$$\Delta M'' = \frac{d(\Delta I_r)}{d\varphi} \frac{\omega^2_{min}}{2} \quad .. \quad .. \quad (5)$$

Let us further show that the values on the right-hand side of equations (4) and (5) can always be determined without plotting a graph of reduced inertia moments, but merely from data obtained by a preliminary kinetic calculation of the mechanism.

In fact, the quantity ΔI_r is known (5) to equal

$$\Delta I_r = \sum_1^n \left[m_1 \left(\frac{v_{s1}}{\omega} \right)^2 + I_1 \left(\frac{\omega_1}{\omega} \right)^2 \right] \quad .. \quad (6)$$

where m_1 and I_1 are mass and moment of inertia of an i–th link of the mechanism; v_{s1} and ω_1 are the velocity of the centre of gravity S_1 and angular velocity of this link. From equation (6) we get

$$\frac{d(\Delta I_r)}{d\varphi} = \frac{2}{\omega^*} \sum_1^n \left[m_{r1} l^2 \frac{a^\tau_{s1}}{v_{s1}} + I_{r1} \frac{\epsilon_1}{\omega_1} \right] .. \quad (7)$$

where m_{r1} is reduced mass of the i–th link; I_{r1} is reduced moment of inertia; 1 is the length of the reduction link; $a^\tau_{s_1}$ is the tangential acceleration of the centre of gravity S_1; ϵ_1 is the angular acceleration of the i-th link assuming that the angular velocity ω^* rests invariable its value in (7) being either ω_{max} or ω_{min}.

It may easily be seen that the ratios $\frac{a^\tau_{s1}}{v_{s1}}$ and $\frac{\epsilon_1}{\omega_1}$ can be replaced by the respective intercepts taken from the velocity and acceleration diagrams. The values of these ratios are positive or negative according to the direction of the vectors $\overline{a^\tau_{s_1}}$, $\overline{v_{s1}}$, $\overline{\epsilon_1}$ and $\overline{\omega_1}$, yet their magnitude ratio

for every position of the mechanism is solely a function of the driving link's rotation angle φ.

Substituting in (4) and (5) the value of the differential quotient (7) we have

$$\Delta M' = \omega_{max} \sum_1^n \left[m_{r1} l^2 \left(\frac{a^\tau_{s1}}{v_{s1}} \right) + I_{r1} \left(\frac{\epsilon_1}{\omega_1} \right) \right] \quad .. \quad (8)$$

$$\Delta M'' = \omega_{min} \sum_1^n \left[m_{r1} l^2 \left(\frac{a^\tau_{s1}}{v_{s1}} \right) + I_{r1} \left(\frac{\epsilon_1}{\omega_1} \right) \right] \quad .. \quad (9)$$

As the quantities under Σ in these equations are equal, the functions $\Delta M'$ and $\Delta M''$ differ only in constant coefficients ω_{max} and ω_{min}. Consequently, by plotting the first function we also obtain the plot of the second to the scale $\mu = \omega_{max}/\omega_{min}$.

Let us now proceed to the determination of flywheel inertia when the coefficient of motion unsteadiness δ and the mean angular velocity ω_{mean} of the driving link are given.

We plot in an ordinary way the diagram of tangential forces or moments $M_d = f(\varphi)$ for the driving link as a function of its rotation angle φ (see Fig. 1). This plot corresponds to one full cycle of the steady motion period. Taking the area of this diagram with a planimeter we find the work of driving forces for a full cycle (in the present case a full cycle is supposed to be equal to 2π). We have

$$A_d = \int_0^{2\pi} M_d \, d\varphi$$

Assuming, as is usual in engineering designs, that the work of resistance forces is constant, we obtain the mean moment of resistance M_r from the equation

$$M_r = \frac{\int_0^{2\pi} M_d \, d\varphi}{2\pi}$$

The curve obtained in the co-ordinate system $O'\Delta M\varphi'$ is that of the excess moment $\Delta M = \Phi(\varphi)$ as defined by equation (3).

By means of equations (8) and (9) we will determine $\Delta M' = F(\varphi)$ and $\Delta M'' = \Psi(\varphi)$. This may be done by substituting ω_{max} and ω_{min} with their values expressed by coefficient δ and by the mean angular velocity ω_{mean}[5]. We have

$$\Delta M' = \omega_{mean} \left(1 + \frac{\delta}{2} \right) \sum_1^n \left[m_{r1} l^2 \left(\frac{a^\tau_{s1}}{v_{s1}} \right) + I_{r1} \left(\frac{\epsilon_1}{\omega_1} \right) \right]$$

$$\Delta M'' = \omega_{mean} \left(1 - \frac{\delta}{2} \right) \sum_1^n \left[m_{r1} l^2 \left(\frac{a^\tau_{s1}}{v_{s1}} \right) + I_{r1} \left(\frac{\epsilon_1}{\omega_1} \right) \right]$$

The function $\Delta M' = F(\varphi)$ thus obtained is plotted on an equal scale (dotted line in the figure) with the diagram $\Delta M = \Phi(\varphi)$. Obviously, the driving link will have a maximum angular velocity at those positions of the mechanism for which $\Delta M' = \Delta M$, that is when the positions a', b', c', and d' are such that the curves $\Delta M = \Phi(\varphi)$ and $\Delta M' = F(\varphi)$ intersects at points a, b, c, and d (see Fig. 1).

Examination of Fig. 1 will show that when the position of the mechanism is at a' or c', the angular velocities ω_{max} cannot possibly be at maximum, as the increment of the kinetic energy in the interval $e'a'$ is less than that of the sum of kinetic energies in the intervals $O'e'$ and $O'h'$, and also less kinetic energy is acquired in the interval $g'c'$ than in $f'g'$.

Therefore in the positions a' and c' we shall have some arbitrary minimum angular velocities which need not however be considered at this juncture. It is

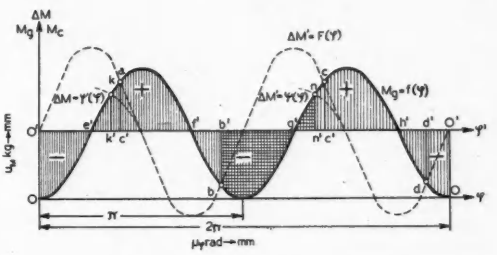

Fig. 1.

apparently in the positions b' and d' that the driving link will reach maximum angular velocities. Just which of these two positions will correspond to the extreme value of angular velocity is a question that may be solved in the customary way by comparing the areas comprised between these values. Suppose that the extreme value ω_{max} corresponds to the positions at b'. Seeing, further, that the functions $\Delta M'' = \Psi(\varphi)$ and $\Delta M' = F(\varphi)$ differ in nothing but scale, the former can be plotted from the diagram of the latter by merely reducing the ordinates in the ratio $\mu = \frac{2-\delta}{2+\delta}$

The plotting of $\Delta M'' = \Psi(\varphi)$ can be dispensed with for the whole range of the angle φ equal to 2π, since it is seen from the plot of $\Delta M' = F(\varphi)$ that in the positions a' and c' the angular velocity of the driving link takes some arbitrary maximum values. Because of the smallness of δ, the true position of the driving link, in which it has minimum angular velocities ω_{min}, must obviously be somewhere near the points a' and c'. It is therefore sufficient to find several points of this curve in the vicinity of a' and c' including, of course, the position in which the function $\Delta M'' = \Psi(\varphi)$ intersects with $\Delta M = f(\varphi)$. These portions of the curve, comprising the intersection points k and n are shown in Fig. 1. It will be obvious that at k' and n' the velocity of the driving link is a minimum because for these positions $\Delta M'' = \Delta M$. Further, we may use the previous method to find the position in which the angular velocity takes the extreme value. Let this position be at n'. Then the moment of inertia of the flywheel I_o is determined from the equation

$$I_o = \frac{2\int_{\varphi_{min}}^{\varphi_{max}} \Delta M \, d\varphi - I_{r\,max}\,\omega^2_{max} - I_{r\,min}\,\omega^2_{min}}{\omega^2_{max} - \omega^2_{min}} \quad (10)$$

where φ_{max} and φ_{min} are the rotation angles of the reduction link corresponding to the points b' and n'; $I_{r\,max}$ and $I_{r\,min}$ are, respectively, the reduced moments of inertia of the mechanism links (without flywheel) corresponding to the above angles φ_{max} and φ_{min}. If $I_{r\,max}$ and $I_{r\,min}$ are small, the following approximate expression may be used, to wit :—

$$I_o \cong \frac{\int_{\varphi_{min}}^{\varphi_{max}} \Delta M \, d\varphi}{\delta\,\omega^2_{mean}} \quad .. \quad .. \quad (11)$$

It should be noted that the problem of determining the functions $\Delta M' = F(\varphi)$ and $\Delta M'' = \Psi(\varphi)$ can be solved equally well by the customary kinetostatic method without computing the derivative of the reduced moment of inertia of the link of the mechanism. In fact,

the second term of the right hand side of equation (3) taken with reverse sign actually represents the moment of all inertia forces of the mechanism reduced to the driving link which is supposed to move with constant velocity(6).

The function $\Delta M' = F(\varphi)$ can be found by ordinary methods of kinetostatics whereby the forces of inertia of individual links are determined on the assumption that the driving link revolves with a constant angular velocity equal to ω_{max}; the reduction of the forces of inertia to the driving link is made by means of the rigid lever theorem. Function $\Delta M'' = \Psi(\varphi)$, as has been mentioned above, will be found by simple conversion of the scale. To conclude it is well to point out that once the moment of inertia of the flywheel has been determined and we have found the positions b' and n' in which the velocity of the driving link takes the values ω_{max} and ω_{min}, respectively, the angular velocity ω_p' of the driving link in any position p' can be determined from the equation

$$\omega_p' = \sqrt{\frac{I_o + m_{rb}' l^2}{I_o + m_{rp}' l^2}\omega^2_{max} - \frac{2}{I_o + m_{rp}' l^2}\int_{\varphi_p'}^{\varphi_b'} \Delta M \, d\varphi} \quad (12)$$

The quantities m_{rp}' and m_{rb}' are reduced masses of the mechanism link in the respective positions p' and b'.

REFERENCES

1 F. Radinger, *Dampfmaschinen mit hoher Kolbengeschwindigkeit* Wien, 1892.
2 F. Wittenbauer, *Graphische Dynamik*, Berlin, 1923.
3 N. I. Mertsalov, *Dinamika mechanismov*, Moscow, 1916.
4 E. M. Gutjar, *Vestnik Metalloprom.*, No. 3, 1939.
5 I. I. Artobolevsky, *Teoria mechanismov i machin*, Moscow, 1940.
6 N. E. Zhukovskii, *Mat. Sborn. Mosk. Matem. ob-va*, 1911.

THERMAL STRESSES IN DISCS.

By E. PALMBLAD. (From *Teknisk Tidskrift*, Vol. 74, 1944, pp. 1345-1347).

INCREASED application of electric welding has stimulated greater interest in the thermal stresses caused by the localised heating of the material in the welding process. In the general case, heat stresses are triaxial and therefore difficult of mathematical treatment. However, in the case of a disc or plate the temperature across the thickness of the material may be considered constant thus reducing the temperature distribution to a problem in two dimensions, that is, in a plane. A further simplification of the problem is obtained by assuming the temperature distribution to be symmetrical with respect to a centre of rotation as will be shown below.

The extension of the disc may be assumed to be so large relative to the temperature field that from the analytical point of view it may be accepted as infinitely large. Point 0 (Fig. 1) which is taken to represent the centre of rotation, is assumed to constitute the point of highest temperature, with the temperature rapidly decreasing with the distance from point 0.

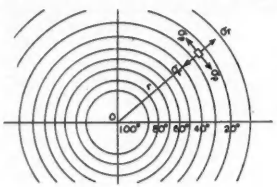

Fig. 1.
Temperature drop, radial, and peripheral stresses.

The general expressions for the elastic deformation of a body of rotation are:

$$\left.\begin{aligned}\frac{\partial^2\xi}{\partial x^2} + \frac{m-2}{2(m-1)} \cdot D\frac{\partial\xi}{\partial r} + \frac{m}{2(m-1)} \cdot \frac{\partial}{\partial x} D\rho - \\ - \frac{m+1}{m-1} \cdot \alpha \cdot \frac{\partial t}{\partial x} = 0\end{aligned}\right\} (1)$$

$$\left.\begin{aligned}\frac{\partial}{\partial r} D\varrho + \frac{m-2}{2(m-1)} \frac{\partial^2\rho}{\partial x^2} + \frac{m}{2(m-1} \cdot \frac{\partial^2\xi}{\partial r \partial x} - \\ \frac{m+1}{m-1} \cdot \alpha \cdot \frac{\partial t}{\partial r} = 0\end{aligned}\right\} (2)$$

$$\sigma_x = \frac{2G}{m-2}\left[(m-1)\frac{\partial\xi}{\partial x} + D\rho - (m+1)\alpha t\right] \quad (3)$$

$$\sigma_r = \frac{2G}{m-2}\left[\frac{\partial\xi}{\partial x} + (m-1)\frac{\partial\rho}{\partial r} + \frac{\rho}{r} - (m+1)\alpha t\right] \quad (4)$$

$$\sigma_p = \frac{2G}{m-2}\left[\frac{\partial\xi}{\partial x} + (m-1)\frac{\rho}{r} + \frac{\partial\rho}{\partial r} - (m+1)\alpha t\right] \quad (5)$$

where ξ and ρ are the elastic deformations in the directions x and r respectively, m is Poisson's ratio, G is the modulus of shear, and σ_x, σ_r, and σ_p are the stress components, t is the temperature in deg. C. at the distance r from the axis of rotation, α is the coefficient of thermal expansion, and $D = \left(\frac{\partial}{\partial r} + \frac{1}{r}\right)$. The dimension of length is given in (cm.), and the stresses in (kg./sq. cm.). In the case of a disc it is $\sigma_x = 0$, and equation (3) therefore becomes

$$\frac{\partial\xi}{\partial x} = -\frac{1}{m-1}\left(\frac{\partial\rho}{\partial r} + \frac{\rho}{r}\right) + \frac{m+1}{m-1} \cdot \alpha \cdot t \quad (3a)$$

Combining the equations (3a), (4), and (5) it follows:

$$\sigma_r = \frac{2G}{m-1}\left[m\frac{\partial\rho}{\partial r} + \frac{\rho}{r} - (m+1)\alpha t\right] \quad (4a)$$

$$\sigma_p = \frac{2G}{m-1}\left[\frac{\partial\rho}{\partial r} + m\frac{\rho}{r} - (m+1)\alpha t\right] \quad (5a)$$

In the case of a disc it is $\frac{\partial\rho}{\partial x} = 0$, and the second term of equation (3a) therefore is also zero. On the basis of equation (3a) it is also

$$\left.\begin{aligned}\frac{\partial^2\xi}{\partial r\,\partial x} = -\frac{1}{m-1}\frac{\partial^2\rho}{\partial r^2} + \frac{1}{r} \cdot \frac{\partial\rho}{\partial r} - \frac{\rho}{r^2} + \\ \frac{m+1}{m-1}\alpha\frac{\partial t}{\partial r}\end{aligned}\right\} (6)$$

and equation (2) therefore can be written

$$\frac{\partial^2\rho}{\partial r^2} + \frac{1}{r}\frac{\partial\rho}{\partial r} - \frac{\rho}{r^2} - \frac{m+1}{2m-1} \cdot \alpha \cdot \frac{\partial t}{\partial r} = 0 \quad (2a)$$

The temperature function $t = f(r)$ contained in equation (2a) will be assumed to be

$$t = t_o\, e^{-hr^2} \quad .. \quad .. \quad .. \quad (7)$$

where t_o is the temperature prevailing at 0; h is a coefficient, and e is the base of the natural logarithm. A typical temperature distribution curve, using $t_o = 100$ deg. C. and $h = 0.05$ cm.$^{-2}$, is charted in Fig. 2. By forming the derivative of equation (7) and introducing into equation (2a) we obtain:

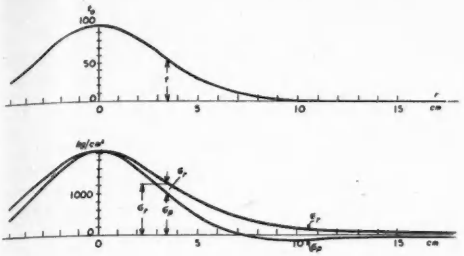

Fig. 2. **Temperature distribution according to $t = t_o\, e^{-0.05\, r^2}$ and corresponding stress curves.**

$$\frac{\partial^2 \rho}{\partial r^2} + \frac{1}{r}\frac{\partial \rho}{\partial r} - \frac{\rho}{r^2} + 2\, t_o\, h\, \frac{m+1}{2m-1} \cdot \alpha\, r\, e^{-hr^2} = 0 \qquad (2b)$$

This is an ordinary differential equation which can therefore be written :

$$d\left(\frac{d\rho}{dr}\right) + \frac{r\, d\rho - \rho\, dr}{r^2} + \frac{m+1}{2m-1} \cdot \alpha \cdot 2 t_o h r e^{-hr^2} \cdot dr = 0$$

By integration we obtain

$$\frac{d\rho}{dr} + \frac{\rho}{r} - \frac{m+1}{2m-1} \cdot \alpha \cdot t_o \cdot e^{-hr^2} + C_1 = 0$$

and by multiplying by $r \cdot dr$

$$r\, d\rho + \rho\, dr - \frac{m+1}{2m-1}\, \alpha \cdot t_o \cdot e^{-hr^2} \cdot r dr + C_1\, r dr = 0$$

and integrating again

$$\rho r + \frac{m+1}{2m-1}\, \alpha \cdot t_o \cdot \frac{e^{-hr^2}}{2h} + C1\, \frac{r^2}{2} + C_2 = 0$$

By dividing by r, we now obtain

$$\rho = -C_1\, \frac{r}{2} - \frac{C2}{r} - \frac{m+1}{2m-1}\, \alpha\, t_o\, \frac{e^{-hr^2}}{2hr}$$

For $r = \infty$ it is $\rho = 0$ and therefore $C1 = 0$. Thus

$$\rho = -\frac{1}{r}\left(C_2 + \frac{m+1}{2m-1}\, \alpha\, t_o\, \frac{e^{-hr^2}}{2h}\right)$$

But it must also be $\rho = 0$ if $r = 0$, and therefore

$$C_2 = -\frac{m+1}{2m-1}\, \frac{\alpha\, t_o}{2h}$$

Introducing this value into the expression for ρ, we obtain

$$\rho = \frac{1}{r}\, \frac{m+1}{2m-1}\, \frac{\alpha\, t_o}{2h}\, (1 - e^{-hr^2}) \quad .. \quad (9)$$

By combining equation (9) with equations (4a) and (5a) respectively we obtain

$$\sigma_r = -\frac{2\, G\, (m+1)\, \alpha}{2m-1}\left(t + \frac{t_o - t}{2\, hr^2}\right) \quad .. \quad (10)$$

$$\sigma_p = -\frac{2\, G\, (m+1)\, \alpha}{2m-1}\left(2t - \frac{t_o - t}{2\, hr^2}\right) \quad .. \quad (11)$$

For large values of r the bracketed factors become negligibly small while for $r = O$ they become 0:0. This indefinite case can be solved by means of equation (7) which yields a value of $\frac{t_o}{2}$. This means that for $r = O$ the stress components σ_r and σ_p become equal, having a value of

$$\sigma_r = \sigma_p = -\frac{3\, G\, (m+1)\, \alpha\, t_o}{2m-1} \quad .. \quad (12)$$

By introducing the following numerical values

G 810,000 kg./sq. cm.
$M = 10/3$
$\alpha = 0.000011$

and by assuming a temperature rise of 100 deg. C. at point 0 over the ambient temperature, we obtain

$$\sigma_r = \sigma_p = -3 \cdot 810{,}000 \cdot 0.000011 \cdot 100 \cdot 3/17 = -2{,}044 \text{ kg./sq. cm.}$$

This result is rather surprising insofar as it shows that the relatively small temperature rise of 100 deg. C. leads to stresses approaching the yield point of the material. If the temperature rise amounts to 200 deg. C., the yield point should therefore be well exceeded and the material deformed by compression.

Furthermore, a subsequent decrease in temperature will cause large tensile stresses in the material.

The stress distribution for $h = 0.05$ cm.$^{-2}$ and $t_o = 100$ deg. C. is charted in Fig. 2, where the temperature distribution is also shown.

Analogous stress distribution curves have been computed for two different temperature functions, to wit :—

(*a*) Linear temperature characteristic, the temperature falling from t_o to 0 deg. C. over the range from $r = O$ to $r = r_1$ (Fig. 3).

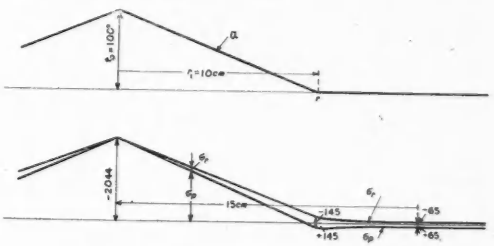

Fig. 3. **Temperature distribution according to $t = t_o\ (1 - x/r)$ for $0 < r < r_1$ and $t = 0$ for $r_1 < r < \infty$ and corresponding stress curves.**

(*b*) Constant temperature t_o between $r = O$ and $r = r_1$, and $t = 0$ from $r = r_1$ to $r = \infty$. In this case integration has to be carried out in two stages, and four integration constants must therefore be determined in both cases. The following relations are available for this purpose, namely $\rho = O$ for $r = O$, and $\rho = O$ for $r = \infty$.

For the border condition where $r = r_1$, the respective ρ and σ_r values computed for either interval must be equal. For point $r = O$ we obtain

$$\sigma_r = \sigma_p = -\frac{3\, G \cdot \alpha \cdot t_o\, (m+1)}{2m-1}$$

and for $r = r_1$ we have

$$\frac{\sigma_r}{\sigma_p} = \frac{-\, G\, \alpha\, t_o\, (m+1)}{+\, 3\, (2m-1)}$$

For a value of $t_o = 100$ deg. C. (Fig. 3) the numerical values of the stresses are

$$\sigma_r = \sigma_p = -2{,}044 \text{ kg./sq. cm.}$$

and

$$\frac{\sigma_r}{\sigma_p} = \frac{-}{+} 145 \text{ kg./sq. cm.}$$

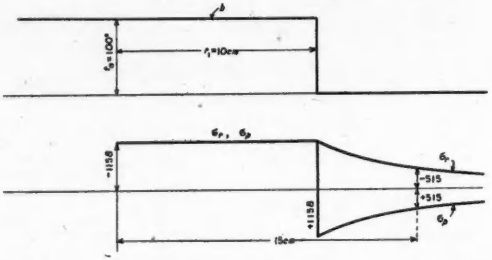

Considering the temperature distribution curve shown in Fig. 4, it is $0<r<r_1$ and

$$\sigma_r = \sigma_p = -G \cdot \alpha \cdot t_0 \frac{m+1}{m} = -1{,}158 \text{ kg. sq. cm.}$$

Fig. 4. Temperature distribution according to $t = t_0$ for $0 < r < r_1$ and $t = 0$ for $r_1 < r < \infty$ and corresponding stress curves.

CERAMIC INSULATING MATERIALS AT HIGH TEMPERATURES.

By F. BELDI. (From *Brown Boveri Review*, Vol. 30, 1943, Nos. 9–10, p. 248.)

PORCELAIN, which is the best-known ceramic insulating material, suffers from the disadvantage that it is not able to withstand the combined effect of high temperature and high electrical stress. The dielectric losses in the insulation of electrical machines and apparatus in most cases are so insignificant from the aspect of electric power consumption that no attention was paid to this matter for many years. The investigation of porcelains subjected to temperatures above 100 deg. C. shows, however, an entirely new picture. Table I lists the electrical constants for quartz and for a few allied ceramic materials used in electrical engineering.

Material	tan δ		ε		ε . tan δ	
	100°	200°	100°	200°	100°	200°
Porcelain I	0.29	2.9	8.0	50	2.32	145
Porcelain II	0.25	2.8	8.2	24	2.04	67
Steatite	0.08	1.4	6.5	12	0.52	17
Calite I	0.010	0.160	5.5	6.5	0.055	1.05
Calite II	0.005	0.013	6.8	6.9	0.034	0.09
Quartz	0.001	0.018	3.2	3.3	0.003	0.06

It will be seen that in the case of the porcelains I and II, which differ only in the proportions of their constituents—china clay, felspar and quartz—the dielectric losses increase very rapidly when the temperature rises from 100 to 200 deg. C. An insulator cube of porcelain II with a volume of 0.1 m³, for instance, which is subjected to a field stress of 1 kV./mm. and has a loss coefficient of $\epsilon \tan \delta = 67$ at 200 deg. C., causes a loss of 185 w. at a frequency of 50 cycles—that is to say, it can almost be looked upon as a heating element.

The magnesium silicate product "steatite" has much better properties in this respect. Finally, the different qualities of calite (listed in Table I), which is a particularly pure magnesium silicate, according to the degree of purity, yield nearly the low values of quartz.

In Fig. 1 the logarithm of the loss coefficient for calite I and II is charted as a function of the test temperature. Particular interest attaches to the sharp bend near the bottom of each curve, which shows that a sudden change takes place at a temperature depending upon the chemical constitution of the material. It will also be noted that in the high temperature range the loss coefficients of the two materials differ by no less than three orders of magnitude.

The high dielectric losses occurring in porcelain at high temperature result in considerable heating of the material, which heating in turn causes a further increase in dielectric losses. Unless adequate arrangements are made for dissipating the heat developed, this phenomenon may lead to thermal destruction of the insulator and hence to breakdowns. The dielectric loss coefficients, which may vary with the temperature, in the higher temperature ranges have, therefore, a most decisive influence upon breakdown strength of the material.

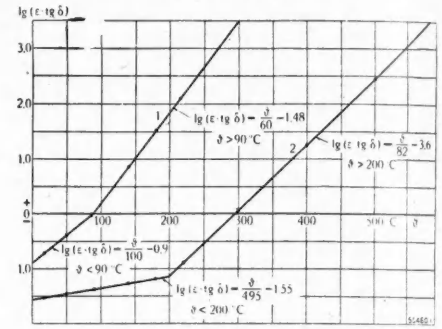

Fig. 1.

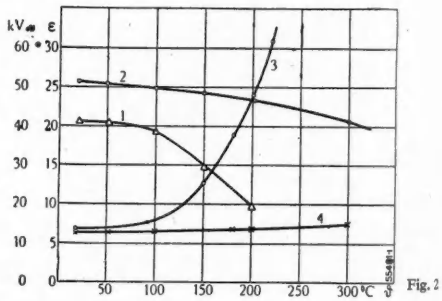

Fig. 2

1 and 2 are over voltages of the porcelain and calite bushings respectively. 3 and 4 dielectric constants of the porcelain and calite bushings respectively.

Apart from the puncturing voltage attention must also be paid to the arc-over voltage. The results of measurements made on bushings of calite and porcelain are charted in Fig. 2. They show the existence of an inter-relation between arc-over voltage and dielectric constant ϵ, a large increase resulting in a considerable decrease in the arc-over voltage. Evaluation of the curve leads to the relationship $E_G \approx \frac{K}{\sqrt{\epsilon}}$ where E_g denotes the voltage at which the first discharges—so-called creep sparks—begin to take place along the surface of the insulator. If the voltage is slightly increased, these discharges lead to breakdown. The factor K is a constant, its value depending upon the geometrical dimensions of the insulator. This relationship holds true as long as the creep voltage is smaller than the arc-over voltage through the air gap.

RADIAL AND LATERAL REACTIONS ACTING UPON THE WHEELS OF A MOTOR CAR

(From E. A. TSUDAKOV's Book, *Theory of the Automobile*, Moscow, 1944, p. 66-81).

IN order to determine the lateral reactions Y_1 and Y_2 acting upon front and rear axle respectively of a motor car passing through a curve, it is necessary to find the forces of inertia to be applied to the centre of gravity of the automobile in order to establish equilibrium. For the purpose of finding these forces of inertia an equation must be established which yields the acceleration prevailing at the centre of gravity. The diagram given in Fig. 1 indicates the travel of an automobile making a turn. Turning is carried out by bringing the front wheels of the automobile into the appropriate position by means of the steering wheel. Actually when turning the steering wheel, the inner and outer wheel of the front axle are turned by slightly different angles, the inner wheel (nearest the centre of rotation) being turned by a slightly greater angle. However, the difference between the two angles is very slight with the usual radius of turn, and a common angle may therefore be assumed in the following investigation, which angle α is the arithmetical means of the individual angles of the two wheels.

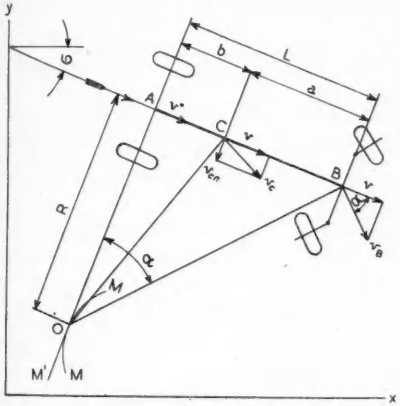

Fig. 1. **Diagram of motion of car making a turn.**

According to Fig. 1 the angle α determines the direction of the speed v_B of the point B which is the centre of the front axle with respect to the longitudinal axis AB of the vehicle. The speed v_A in point A, which is the centre of the rear axle, is in the direction of the longitudinal axis AB and equals the speed v prevailing at the centre of gravity located at point C. In the following analysis the speed v will be termed the *motion of the automobile*.

The investigation of the motion of the automobile will be based upon the assumption that neither of its axles skids sideways and that no lateral movement of the axle is caused by a lateral deformation of the tyres. Thus the path of travel of the automobile will correspond to the swinging of the travelling centroid AM' on the fixed centroid MM. The distance AO between the instantaneous centre of gyration O of the vehicle and the longitudinal axis AB is termed the *turning radius of the vehicle* and denoted by R. The travel of the automobile is to be examined for a varying length of radius R that is for a varying angle α. One of the problems of the investigation therefore is to establish the relationship between the turning speed $\frac{d\alpha}{dt}$ or the speed of the variation in the radius R—and the lateral stability of the automobile.

Point C in Fig. 1 represents the centre of gravity of the automobile located at the distances a and b from the front and rear axles respectively. The distance between the two axles is given by the length L. The velocity v_C of the centre of gravity is at right angles with the radius OC. This velocity may be replaced by two component velocities, namely the velocity v in line with the longitudinal axis AB of the vehicle, and the velocity v_{cn} the direction of which forms a right angle with AB. Referring to Fig. 1 it will be seen that the following relation exists, to wit :—

$$\frac{v_{cn}}{v_c} = \frac{b}{OC}; \quad v_{cn} = \frac{v_c}{OC} \cdot b = b \cdot \omega \quad .. \quad (1)$$

where ω is the angular turning velocity.

The acceleration of the centre of gravity (point C) can also be replaced by two components of which the tangential acceleration j_{ct} is in the direction of the longitudinal axis AB, while the other component which represents the normal acceleration, encloses an angle of 90 deg. with the longitudinal axis. In order to determine these accelerations we consider the motion of the automobile with respect to the fixed system of coordinates X—Y. In Fig. 1 the angle formed by the length axis of the automobile with the X axis is given by σ, and it therefore can be written :

$$\omega = \frac{d\sigma}{dt}; \quad \frac{d\omega}{dt} = j_w = \frac{d^2\sigma}{dt^2}$$

where $\frac{d\omega}{dt}$ is the angular acceleration of the vehicle.

By expressing the velocity v_c, or its components v and v_{cn}, with respect to the X—Y axes, we find that

$$v_x = v \cdot \cos\sigma - b \cdot \omega \cdot \sin\sigma \quad .. \quad (2)$$

$$v_y = -v \cdot \sin\sigma - b \cdot \omega \cdot \cos\sigma \quad .. \quad (3)$$

By differentiating these equations we obtain an expression for the projected acceleration of point C with respect to the X—Y axes. It is

$$j_{cx} = \frac{dv_x}{dt} = \frac{dv}{dt}\cos\sigma - v \cdot \omega \cdot \sin\sigma - b\frac{d\omega}{dt}\sin\sigma - b\,\omega^2\cos\sigma \quad .. \quad (4)$$

$$j_{cy} = \frac{dv_y}{dt} = b \cdot \omega^2 \cdot \sin\sigma - b\frac{d\omega}{dt}\cos\sigma - \frac{dv}{dt}\sin\sigma - v\omega\cos\sigma \quad .. \quad (5)$$

Referring to Fig. 2 it is seen that j_{cx} and j_{ct} can also be

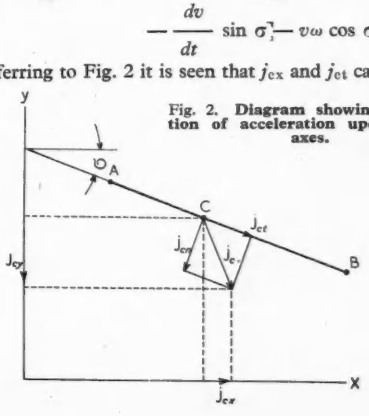

Fig. 2. **Diagram showing projection of acceleration upon X — Y axes.**

obtained as the projections of j_{ct} and j_{cn} upon the respective axes, and we have

$$j_{cx} = j_{ct} \cos \sigma - j_{cn} \sin \sigma \quad .. \quad (6)$$

$$- j_{cy} = j_{ct} \sin \sigma - j_{cn} \cos \sigma \quad .. \quad (7)$$

By combining these expressions with the equations (4) and (5) and solving for j_{ct} and j_{cn} we obtain

$$j_{ct} = \frac{dv}{dt} - b \cdot \omega^2 \quad .. \quad .. \quad .. \quad (8)$$

$$j_{cn} = \omega \cdot v + b \frac{d\omega}{dt} = \omega^2 R + b \frac{d\omega}{dt} \quad (9)$$

We have thus obtained the tangential and the normal accelerations of the centre of gravity as they prevail during turning of the vehicle, assuming that no lateral skidding takes place.

According to equation (8) the tangential acceleration which acts along the longitudinal axis of the car is given by the tangential acceleration $\frac{dv}{dt}$ at point A minus the centripetal acceleration $b \cdot \omega^2$ existing at point C relative to point A. Considering equation (9) it is seen that the normal acceleration is given by the centripetal acceleration $\omega^2 R$ at point A augmented by the tangential acceleration $b \cdot \frac{d\omega}{dt}$ existing at point C with respect to point A.

The absolute values of the forces of inertia can therefore be established as follows:

Tangential force of inertia:

$$T = M \cdot j_{ct} = M \left(\frac{dv}{dt} - b \cdot \omega^2 \right) \quad .. \quad (10)$$

Normal force of inertia:

$$N = M \cdot j_{cn} = M \left(\omega^2 R + b \frac{d\omega}{dt} \right) \quad .. \quad (11)$$

where M is the mass of the vehicle.

The various forces acting upon the vehicle when turning are indicated in Fig. 3. In order to establish the condition of equilibrium we introduce the moment of inertia

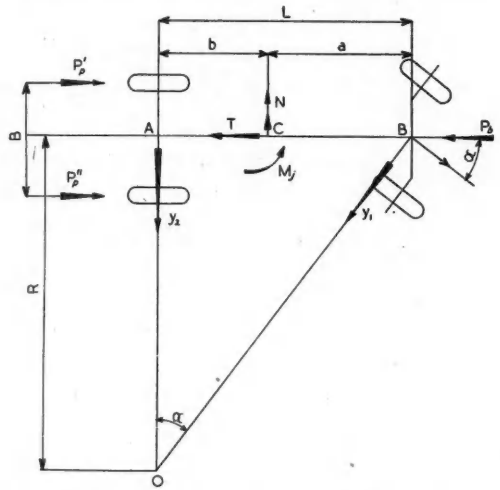

Fig. 3. **Diagram of forces acting upon car making a turn.**

$$Mj = M \cdot \rho^2 \frac{d\omega}{dt}, \quad .. \quad .. \quad (12)$$

where ρ is the radius of gyration with respect to the vertical axis passing through the centre of gravity C. We further introduce the tractive forces P_p' and P_p'' acting upon the outer and inner wheel of the rear axle respectively. We also introduce the lateral reactions Y_1 and Y_2 acting upon front and rear axle, and the force P_b which resists the motion of the vehicle. This force is the sum total of the force resisting the rolling of the wheels and of the air resistance. For practical purposes it will be sufficiently accurate to assume that the resisting force P_b acts along the line of symmetry of the vehicle.

From the condition of equilibrium of the moments acting upon vertical axis through point A we obtain

$$Y_1 \cdot L \cdot \cos \alpha = N \cdot b + Mj + M_f + (P_p'' - P_p') \frac{B}{2}$$

If $P_p = P_p' - P_p''$ represents the total propulsive force, and if

$$k = \frac{P_p''}{P_p}, \text{ it will be } P_p' = (1 - k) P_p$$

By further introducing

$$P_p = \gamma_p \cdot G = \gamma_p \cdot g \cdot M,$$

and also introducing the expressions for N and Mj given in equations (11) and (12) respectively, we then find

$$Y_1 \cdot \cos \alpha = \frac{M \cdot b}{L} \left[\omega^2 \cdot R + \left(b + \frac{\rho^2}{b} \right) \frac{d\omega}{dt} \right] - \gamma_p \cdot g \cdot M (2k - 1) \frac{B}{2L} \quad .. \quad .. \quad (13)$$

Similarly, by establishing the condition of equilibrium for the vertical axis passing through point B, we find

$$Y_2 = \frac{M \cdot a}{L} \left[\omega^2 \cdot R + \left(b - \frac{\rho^2}{a} \right) \frac{d\omega}{dt} \right] - \gamma_p \cdot g \cdot M (2k - 1) \frac{B}{2L} \quad .. \quad .. \quad (14)$$

By expressing the turning speed ω in terms of the speed v, we obtain

$$\omega = \frac{v}{R}; \quad \frac{d\omega}{dt} = \frac{1}{R} \frac{dv}{dt} - \frac{v}{R^2} \cdot \frac{dR}{dt}$$

According to equation (3) it is

$$L = R \cdot \tan \alpha; \quad \frac{dR}{dt} = - \frac{R^2}{L \cdot \cos^2 \alpha} \cdot \frac{d\alpha}{dt}$$

Therefore

$$\frac{d\omega}{dt} = \frac{1}{R} \frac{dv}{dt} + \frac{v}{L \cdot \cos^2 \alpha} \frac{d\alpha}{dt} \quad .. \quad (15)$$

so that the equations (13) and (14) can now be written thus:

$$Y_1 \cos \alpha = \frac{M \cdot b}{L} \left[\frac{v^2}{R} + \left(b + \frac{\rho^2}{b} \right) \left(\frac{1}{R} \frac{dv}{dt} + \frac{v}{L \cos^2 \alpha} \frac{d\alpha}{dt} \right) + \gamma_p \cdot g (2k - 1) \frac{B}{2b} \right] .. \quad (16)$$

$$Y_2 = \frac{M \cdot a}{L} \left[\frac{v^2}{R} + \left(b - \frac{\rho^2}{a} \right) \left(\frac{1}{R} \frac{dv}{dt} + \frac{v}{L \cos^2 \alpha} \cdot \frac{d\alpha}{dt} \right) - \gamma_p \cdot g (2k - 1) \frac{B}{2\alpha} \right] .. \quad (17)$$

According to these equations, the lateral reactions Y_1 and Y_2 increase with increasing speed v and increasing acceleration $\frac{dv}{dt}$. They also increase with increasing $\frac{d\alpha}{dt}$ and with a decreasing radius R. Conversely, with a negative value of $\frac{d\alpha}{dt}$, as it occurs when the vehicle has finished its turn and begins to assume straight line travel again, an increase in $\frac{d\alpha}{dt}$ will cause a decrease in the lateral reactions Y_1 and Y_2, that is to say, the stability of the rear axle is increased. Moreover the lateral reactions Y_1 and Y_2 decrease with negative values of the acceleration $\frac{dv}{dt}$, that is, with the vehicle slowing down.

The respective influence of the acceleration $\frac{dv}{dt}$ and the speed $\frac{d\alpha}{dt}$ upon the lateral reactions Y_1 and Y_2, largely depends upon the location of the centre of gravity on the length axis, and also upon the disposition of the mass of the automobile with respect to its length. The location of the centre of gravity is given by the distances a and b, while that of the mass is expressed by the magnitude of the radius of gyration ρ. The relation between the distances a and b, and the radius ρ is a measure of the degree to which the lateral reactions are affected by the acceleration $\frac{dv}{dt}$ and the speed $\frac{d\alpha}{dt}$. If the radius of gyration is $\rho = \sqrt{a \,.\, b}$, both the acceleration $\frac{dv}{dt}$ and the speed $\frac{d\alpha}{dt}$ will be without any influence upon the magnitude of the lateral reaction Y_2, which acts upon the rear axle of the vehicle.

Concerning the influence of an uneven distribution of the tractive force over the driving wheels, equations (16) and (17) show that the transmission of a greater tractive force to the inner wheel ($k>0.5$) causes a noticeable increase in the lateral reaction Y_1 which acts upon the front axle of the car, and a corresponding decrease in the lateral reaction Y_2 exerted upon the rear axle. This variation in the forces of reaction increases with the magnitude of the coefficient γ_p of the force of inertia, and it also increases with the magnitude of the coefficient k which is a measure of the distribution of the tractive force to the wheels.

If the forces of traction are unevenly distributed to the wheels of the rear axle ($k>0.5$) the front axle of the vehicle will display a greater tendency to skidding, and the actual turning radius will therefore be somewhat larger than the radius corresponding to the position of the steering wheel.

On the basis of the balance of the tractive effect, the following expressions for the motion of the automobile on an horizontal surface can be established, to wit :—

$$P_p = \gamma_p \,.\, G = P_w + P_f + P_j = K \,.\, F \,.\, v^2 + f \,.\, G + \frac{\delta}{g} \,.\, G \,.\, \frac{dv}{dt} \quad .. \quad .. \quad .. \quad (18)$$

where $K F v^2$ is the force of air resistance, $f \,.\, G$ is the force of the rolling friction of the wheels, $\left(\frac{\delta}{g}\right) \,.\, G \,.\, \frac{dv}{dt}$ is the force expended upon the acceleration $\frac{dv}{dt}$ of the vehicle, k is the coefficient of air resistance, depending upon the shape of the car, F is the effective frontal surface of the automobile subject to air resistance, f is the coefficient of rolling friction of the wheels, δ is a coefficient which takes account of the revolving masses of the car (flywheel, wheels).

We introduce

$$k \,.\, F = W \text{ and } \frac{W}{G} = Z,$$

where W denotes the factor of air resistance expressed in *kg* and based upon a speed of the car of 1 m. per second.

Z is the specific resistance of the air. By introducing these factors into equation (18) we obtain

$$\gamma_p = Z \,.\, v^2 + f + \frac{\sigma}{g} \frac{dv}{dt} \quad .. \quad .. \quad (19)$$

If the car travels at constant speed, we therefore have

$$\gamma_p = Z \,.\, v^2 + f \quad .. \quad .. \quad (19a)$$

Equations (19) and (19a) apply to the case of straight line travel. But if the car makes a turn, the following equations will apply. Referring to Fig. 3 it is :

$$P_p = P'_p + P''_p = T + P_b + Y_1 \sin \alpha$$

The force P_b resisting the forward motion of the car is the sum total of the force P_w due to the air resistance and the force P_f due to the rolling friction of the wheels. It therefore is

$$\gamma_p = \frac{P_p}{G} = Z \,.\, v^2 + f + \frac{M}{G} \frac{dv}{dt} + \frac{Y_1 \sin \alpha - M \,.\, b \,.\, \omega^2}{G}$$

By dividing both sides of equation (16) by the weight G_1 carried by the front axle, and also dividing both sides of the equation (17) by the weight G_2 carried by the rear axle, we arrive at the specific lateral reactions $\frac{Y_1}{G_1}$ and $\frac{Y_2}{G_2}$. We also introduce the expression γ_p (19) into equations (16) and (17) and assume $\cos \alpha = 1$. We then obtain

$$\frac{Y_1}{G_1} = \frac{v^2}{g \,.\, R} + \left(b + \frac{\rho^2}{b} \right) \left(\frac{1}{g \,.\, R} \,.\, \frac{dv}{dt} + \frac{v}{g \,.\, L} \,.\, \frac{d\alpha}{dt} \right) + + \left(Z \,.\, v^2 + f + \frac{\delta}{g} \frac{dv}{dt} \right) (2k - 1) \frac{B}{2b} \quad .. \quad (20)$$

$$\frac{Y^2}{G_2} = \frac{v^2}{g \,.\, R} + \left(b - \frac{\rho^2}{\alpha} \right) \left(\frac{1}{g.R} \,.\, \frac{dv}{dt} + \frac{v}{g \,.\, L} \,.\, \frac{d\alpha}{dt} \right) - - \left(Z \,.\, v^2 + f + \frac{\delta}{g} \frac{dv}{dt} \right) (2k - 1) \frac{B}{2a} \quad .. \quad (21)$$

If the vehicle travels at constant speed $\left(\frac{dv}{dt} = O \right)$ along a curve of constant radius $\left(\frac{d\alpha}{dt} = O \right)$, the equations (20) and (21) take the form

$$\frac{Y_1}{G_1} = \frac{v^2}{g \,.\, R} + (Z_1 \,.\, v^2 + f) \,.\, (2k - 1) \,.\, \frac{B}{2b} \quad .. \quad (20a)$$

$$\frac{Y_2}{G_2} = \frac{v^2}{g \,.\, R} - (Z \,.\, v^2 + f) \,.\, (2k - 1) \,.\, \frac{B}{2a} \quad .. \quad (21a)$$

Furthermore, if $k = 1$, it will be

$$\frac{Y_1}{G_1} = \frac{v^2}{g \cdot R} + \left(b + \frac{\rho^2}{b}\right) \cdot \left(\frac{1}{g \cdot R} \cdot \frac{dv}{dt} + \frac{v}{g \cdot L} \cdot \frac{d\alpha}{dt}\right) + + \left(Z \cdot v^2 + f + \frac{\delta}{g} \cdot \frac{dv}{dt}\right) \cdot \frac{B}{2b} \quad .. \quad .. \quad (20b)$$

$$\frac{Y_2}{G_2} = \frac{v^2}{g \cdot R} + \left(b - \frac{\rho^2}{a}\right) \left(\frac{1}{g R} \cdot \frac{dv}{dt} + \frac{v}{g \cdot L} \cdot \frac{d\alpha}{dt}\right) - - \left(Z \cdot v^2 + f + \frac{\delta}{g} \cdot \frac{dv}{dt}\right) \cdot \frac{B}{2a} \quad .. \quad .. \quad (21b)$$

But if the coefficient k has a value of $k = 0.5$, that is, if the tractive force P_p is uniformly distributed over the driving wheels, then

$$\frac{Y_1}{G_1} = \frac{v^2}{g \cdot R} + \left(b + \frac{\rho^2}{b}\right) \cdot \left(\frac{1}{g \cdot R} \cdot \frac{dv}{dt} + \frac{v}{g \cdot L} \cdot \frac{d\alpha}{dt}\right) \quad (20c)$$

$$\frac{Y_2}{G_2} = \frac{v^2}{g \cdot R} + \left(b - \frac{\rho^2}{a}\right) \cdot \left(\frac{1}{g \cdot R} \cdot \frac{dv}{dt} + \frac{v}{g \cdot L} \cdot \frac{d\alpha}{dt}\right) \quad (21c)$$

Finally by assuming the car to travel at constant speed $\left(\frac{dv}{dt} = 0\right)$ along a curve of constant radius $\left(\frac{d\alpha}{dt} = 0\right)$ with k having the value $k = 0.5$, we obtain

$$\frac{Y_1}{G_1} = \frac{v^2}{g \cdot R} \quad (20d) \quad \text{and} \quad \frac{Y_2}{G_2} = \frac{v^2}{g \cdot R} \quad (21d)$$

In order to illustrate these various relationships, the lateral reactions $\frac{Y_1}{G_1}$ and $\frac{Y_2}{G_2}$ are shown in Figs. 4-12, both as functions of the physical data of the vehicle (factors $\frac{a}{L}$, $\frac{\rho}{L}$, and k) and of its motion (v, $\frac{dv}{dt}$, $\frac{d\alpha}{dt}$ and R).

Thus, for instance, Figs. 4 and 5 show the specific lateral reactions $\frac{Y_1}{G_1}$ and $\frac{Y_2}{G_2}$ respectively as functions of the speed v for different locations of the centre of gravity on the longitudinal axis of the car. According to equations (20) and (21), the factors $\frac{a}{L}$ and $\frac{\rho}{L}$ affect the lateral reactions only if the car is in non-uniform motion, that is to say, if $\frac{dv}{dt} \gtrless 0$ and $\frac{d\alpha}{dt} \gtrless 0$. With

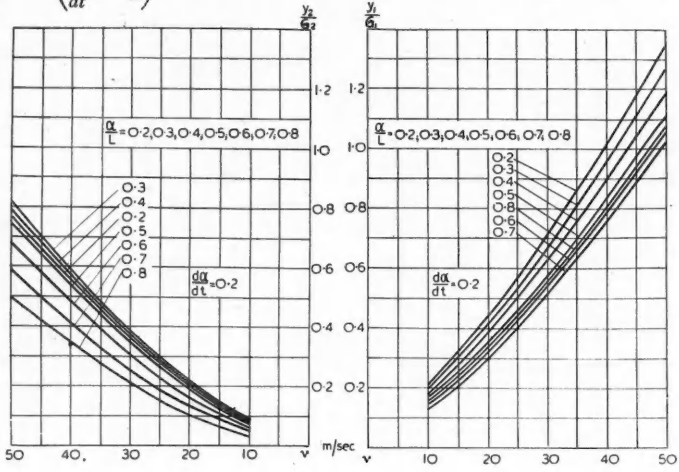

Fig. 4. **Lateral reactions** *vs* **speed** v **for a different value of** $\frac{a}{L}$ **for given positive value of** $\frac{d\alpha}{dt}$.

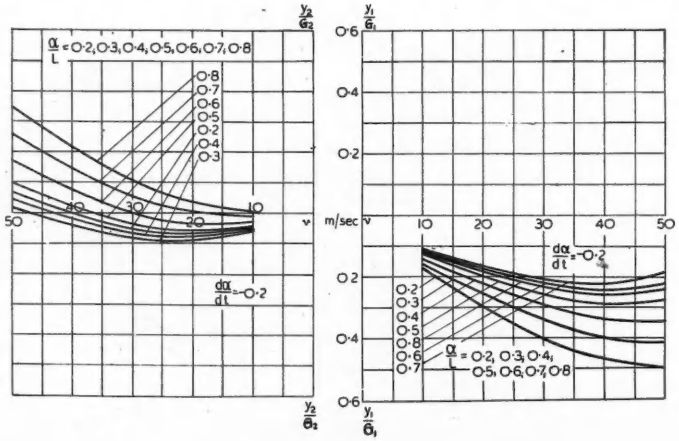

Fig. 5. **Lateral reactions** *vs* **speed** v **for different values of** $\frac{a}{L}$ **for given negative value of** $\frac{d\alpha}{dt}$.

this point in view the graphs Figs. 4 and 5 are based on a value of $\frac{d\alpha}{dt} = 0.2$ rad. per second, and of $\frac{d\alpha}{dt} = -0.2$ rad. per second respectively. As will be seen from Figs. 4 and 5 these charts are based on values for $\frac{a}{L}$ ranging from 0.2 to 0.8. It should also be noted that the charts are based on a coefficient $k = 0.5$, with the equations (20) and (21) taking the form

$$\frac{Y_1}{G_1} = \frac{v^2}{g \cdot R} + \left(L - a + \frac{\rho^2}{L-a} \right) \cdot \frac{v}{g \cdot L} \cdot \frac{d\alpha}{dt} \qquad (20e)$$

$$\frac{Y_2}{G_2} = \frac{v^2}{g \cdot R} + \left(L - a - \frac{\rho^2}{a} \right) \cdot \frac{v}{g \cdot L} \cdot \frac{d\alpha}{dt} \qquad (21e)$$

Referring to the right hand side of Fig. 4 it will be seen that with increasing values of $\frac{a}{L}$, that is to say, with the centre of gravity being shifted towards the rear axle, the specific lateral reaction $\frac{Y_1}{G_1}$ is diminished. But if a certain value for $\frac{a}{L}$ is exceeded, the reaction tends to increase once more. In order to find the value for $\frac{a}{L}$ which yields the minimum lateral reaction $\frac{Y_1}{G_1}$, we differentiate equation (20) with respect to a and obtain

$$\frac{d}{da}\left(\frac{Y_1}{G_1}\right) = \left(\frac{1}{g \cdot R} \cdot \frac{dv}{dt} + \frac{v}{g \cdot L} \cdot \frac{d\alpha}{dt}\right) \frac{d}{da}$$
$$\left(L - a + \frac{\rho^2}{L-a}\right) + \gamma_p (2k - 1) \frac{d}{da} \frac{B}{2(L-a)}$$

or

$$\frac{d}{da}\left(\frac{Y_1}{G_1}\right) = \left(\frac{1}{g \cdot R} \frac{dv}{dt} + \frac{v}{g \cdot L} \cdot \frac{d\alpha}{dt}\right) \cdot \left[\frac{\rho^2}{(L-a)^2} - 1\right] +$$
$$+ \gamma_p \cdot (2k - 1) \cdot \frac{B}{2(L-a)^2}$$

By equating the right hand side to zero, we have

$$(L - a_1)^2 = \rho^2 + \frac{0.5\, \gamma_p\, (2k - 1)\, B}{\frac{1}{g \cdot R} \cdot \frac{dv}{dt} + \frac{v}{g \cdot L} \cdot \frac{d\alpha}{dt}} \qquad (22)$$

where a_1 is the value for a for which the lateral reaction $\frac{Y_1}{G_1}$ attains a minimum.

By making $k = 0.5$ we have

$$L - a_1 = \rho \text{ or } a_1 = L - \rho \quad .. \quad .. \quad (22a)$$

With $\frac{\rho}{L} = 0.3$, therefore $a_1 = 0.7\, L$.

Referring to the left hand side of Fig. 4 it will be seen that with increasing values for $\frac{a}{L}$, the lateral reaction $\frac{Y_2}{G_2}$ at first increases and then decreases. In order to find the value of a_2 of a for which the lateral reaction $\frac{Y_2}{G_2}$ attains its maximum, we establish the first derivative of equation (21) with respect to a and obtain

$$\frac{d}{da}\left(\frac{Y_2}{G_2}\right) = \left(\frac{1}{g \cdot R} \cdot \frac{dv}{dt} + \frac{v}{g \cdot L} \cdot \frac{d\alpha}{dt}\right) \cdot \frac{d}{da}$$
$$\left(L - a - \frac{\rho^2}{a}\right) - \gamma_p \cdot (2k - 1) \cdot \frac{d}{da} \frac{B}{2a}$$

or

$$\frac{d}{da}\left(\frac{Y_2}{G_2}\right) = \left(\frac{1}{g \cdot R} \cdot \frac{dv}{dt} + \frac{v}{g \cdot L} \cdot \frac{d\alpha}{dt}\right) \cdot \left(\frac{\rho^2}{a_2} - 1\right) +$$
$$+ \gamma_p \cdot (2k - 1) \cdot \frac{B}{2a^2} \cdot$$

and by equating to zero :

$$a_2^2 = \rho^2 + \frac{0.5\, \gamma_p \cdot (2k - 1) \cdot B}{\frac{1}{g \cdot R} \cdot \frac{dv}{dt} + \frac{v}{g \cdot L} \cdot \frac{d\alpha}{dt}} \quad .. \quad .. \quad (23)$$

For $k = 0.5$ it therefore will be $a_2 = \rho$ .. (23a)

Again assuming $\frac{\rho}{L} = 0.3$, we have $a_2 = 0.3\, L$.

The graphs shown in Fig. 5 are based on a negative value of $\frac{d\alpha}{dt} = -0.2$ rad. per second. Referring to the right hand side of this graph it is seen that the lateral reaction $\frac{Y_1}{G_1}$ has negative values over the entire range of speeds covered. The lateral reaction $\frac{Y_2}{G_2}$ is likewise negative over a certain range. The reaction $\frac{Y_1}{G_1}$ is seen to pass through a minimum ; this is in accordance with equation (22a).

Figs. 6 and 7 show the relationship between the specific lateral reactions and the speed v of the vehicle for different radii of gyration, these graphs being based on equations (20e) and (21e). It will be noted that Fig. 6 is based on a value of $\frac{d\alpha}{dt} = 0.2$ rad. per second, and Fig. 7 on a corresponding negative value.

According to Fig. 6 an increase in the radius of gyration $\frac{\rho}{L}$ leads to an increase in $\frac{Y_1}{G_1}$ and a decrease in $\frac{Y_2}{G_2}$. This means that a dispersal of the mass of the vehicle relative to the vertical axis passing through the centre of gravity improves the lateral stability of the rear axle and diminishes that of the front axle.

As the rear axle has a greater tendency to skidding than the front axle, an increase in the radius of gyration will, on the whole, have a beneficial effect upon the lateral stability of the vehicle. According to Fig. 7

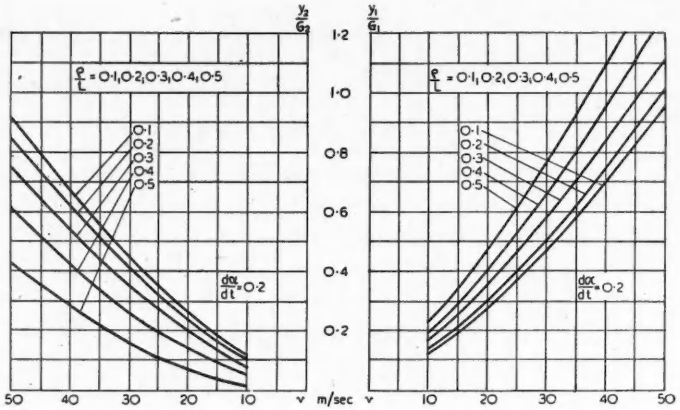

Fig. 6. **Lateral reactions *vs* speed *v* for different radii of gyration $\frac{\rho}{L}$ for given positive value of $\frac{d\alpha}{dt}$.**

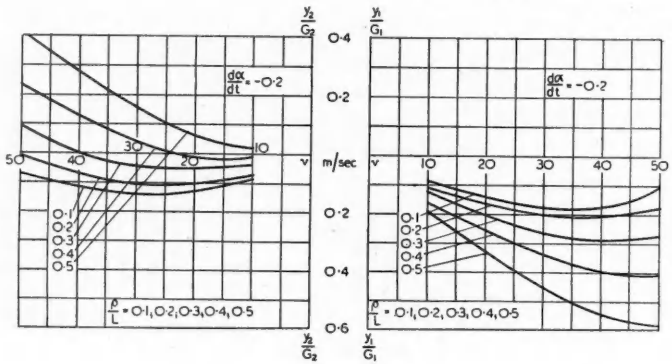

Fig. 7. **Lateral reactions *vs* speed *v* for different radii of gyration $\frac{\rho}{L}$ for given negative value of $\frac{d\alpha}{dt}$.**

negative values of $\frac{d\alpha}{dt}$ will produce negative reactions $\frac{Y_1}{G_1}$ over the entire range of speeds; while the reactions $\frac{Y_2}{G_2}$ considerably diminish and even attain negative values at certain speeds and with small values of $\frac{\rho}{L}$. This is to say, in certain cases the prevailing conditions are analogous with those indicated in the graphs Figs. 4 and 5.

The speeds v of the vehicle for which the curves in the left hand side graphs of Figs. 5 and 7 intersect with the abscissa, can be obtained from equation (21e) by equating $\frac{Y_2}{G_2}$ to zero. We then have

$$v = \frac{R}{L} \cdot \left(L - a - \frac{\rho^2}{a} \right) \left| \frac{d\alpha}{dt} \right|.$$

Fig. 8 shows the relationship between the specific lateral reactions $\frac{Y_1}{G_1}$ and $\frac{Y_2}{G_2}$ and the travelling speed v for different numerical values of the coefficient k. These curves are derived from equations (20a) and (21a), that is, for the case in which $\frac{dv}{dt} = 0$ and $\frac{d\alpha}{dt} = 0$. Referring to Fig. 8 it will be seen that an increase in k causes the lateral reaction $\frac{Y_1}{G_1}$ to increase and the lateral

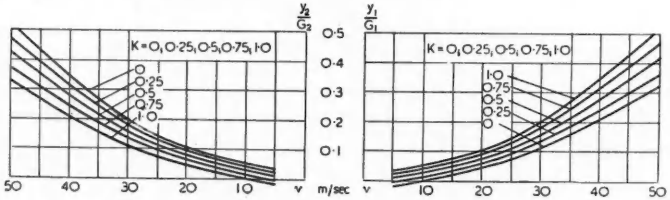

Fig. 8. **Lateral reactions *vs* speed for different values of *k*.**

reaction $\frac{Y_2}{G_2}$ to diminish. It will also be noted that for certain values of k and v both the lateral reactions are zero. In the case of the reaction Y_1 this occurs if $k = 0.5$, and in the case of reaction Y_2 if $k = 0.5$. This fact may also be deduced from equations (16) and (17).

For certain travelling conditions of the automobile, as defined by the speed v and the turning radius R (provided they are coincident with certain values for k), the lateral reactions Y_1 and Y_2 may be zero. The respective co-ordinated values for v and R required to produce a case of this kind can be found from equations (20) and (21). Equating Y_1 to zero in equation (20) and making $\frac{d\alpha}{dt} = 0$, that is, assuming a constant-radius turn, we find

$$R_1^0 = \frac{(v^0) + \left(b + \frac{\rho^2}{b}\right) \cdot \frac{dv^0}{dt}}{g \cdot (1-2k) \cdot \frac{B}{2b} \cdot \left[Z \cdot (v^0)^2 + f + \frac{\delta}{g} \cdot \frac{dv^0}{dt}\right]} \quad (24)$$

which yields the relationship between R_1^0 and v^0 for the case of non-uniform speed of the vehicle. If we assume the vehicle to travel at constant speed, i.e., if $\frac{dv}{dt} = 0$, we find

$$R_1^0 = \frac{2\,b \cdot (v^0)^2}{g \cdot B \cdot (1-2k) \cdot [Z \cdot (v^0)^2 + f]} \quad .. \quad (24a)$$

If $k = 0$, as it may happen whenever the inside wheel of the rear axle encounters a particularly slippery spot of ground, equation (24) will become

$$R_1^0 = \frac{(v^0)^2 + \left(b + \frac{\rho^2}{b}\right) \cdot \frac{dv^0}{dt}}{g \cdot \frac{B}{2b} \cdot \left[Z \cdot (v^0)^2 + f + \frac{\delta}{g} \cdot \frac{dv^0}{dt}\right]} \quad .. \quad (24b)$$

and if it is also assumed that $\frac{dv}{dt} = 0$, equation (24) will then read

$$R_1^0 = \frac{2\,b \cdot (v^0)^2}{g \cdot B \cdot [Z \cdot (v^0)^2 + f]} \quad .. \quad .. \quad (24c)$$

Analogous equations may be established for the rear axle of the car. Thus, by equating Y_2 (equation 21) to zero and making $\frac{d\alpha}{dt} = 0$, we have

$$R_2^0 = \frac{(v^0)^2 + \left(b - \frac{\rho^2}{a}\right) \cdot \frac{dv^0}{dt}}{g \cdot (2k-1) \cdot \frac{B}{2a} \cdot \left[Z \cdot (v^0)^2 + f + \frac{\delta}{g} \cdot \frac{dv^0}{dt}\right]} \quad (25)$$

For the case of constant speed, this equation takes the form

$$R_2^0 = \frac{2\,a \cdot (v^0)^2}{g \cdot B \cdot (2k-1) \cdot [Z \cdot (v^0)^2 + f]} \quad .. \quad (25a)$$

If we introduce $k = 1$ (which is the max. value which it can attain) into equation (25), we have

$$R_2^0 = \frac{(v^0)^2 + \left(b - \frac{\rho^2}{a}\right) \cdot \frac{dv^0}{dt}}{g \cdot \frac{B}{2a} \cdot \left[Z \cdot (v^0)^2 + f + \frac{\delta}{g} \cdot \frac{dv^0}{dt}\right]} \quad .. \quad (25b)$$

and if we further assume the car to travel at constant speed, we obtain

$$R_2^0 = \frac{2\,a \cdot (v^0)^2}{g \cdot B \cdot [Z \cdot (v^0)^2 + f]} \quad .. \quad .. \quad (25c)$$

The graphs shown in Fig. 9 are based on the equations (20e) and (21e) and show the influence of the speed v upon the specific lateral reactions $\frac{Y_1}{G_1}$ and $\frac{Y_2}{G_2}$ for

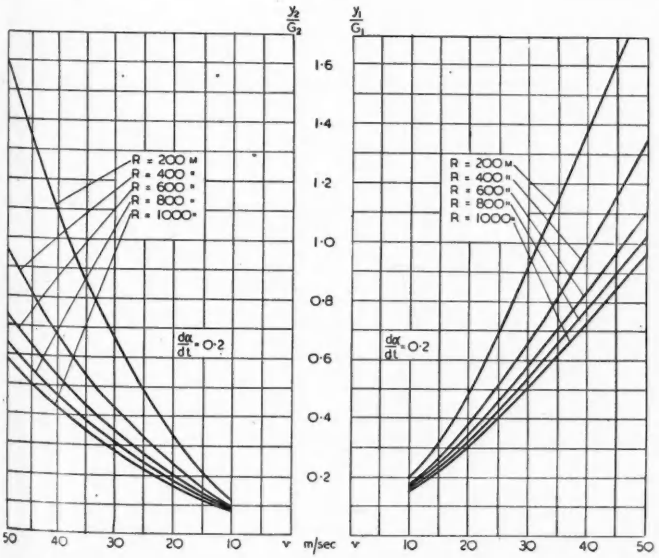

Fig. 9. Lateral reactions *vs* speed v for different turning radius R with constant positive $\frac{d\alpha}{dt}$.

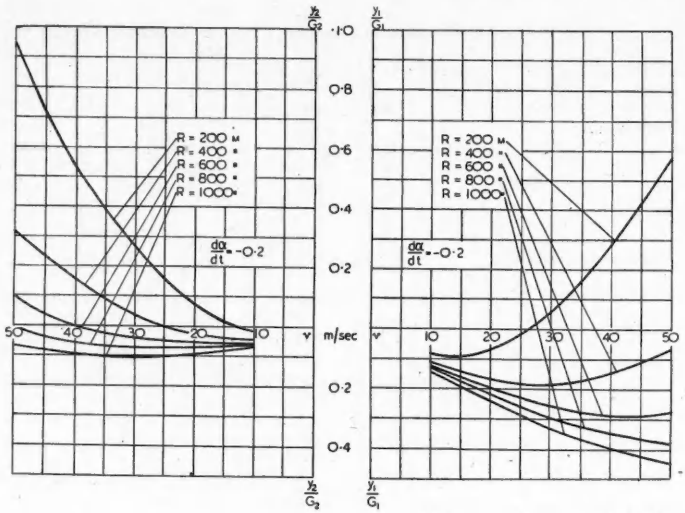

Fig. 10. **Lateral reactions *vs* speed *v* for different turning radius *R* with constant negative $\frac{d\alpha}{dt}$.**

different radii *R*. In this case it is assumed that $\frac{d\alpha}{dt} =$ 0.2 rad. per second. Similar graphs are shown in Fig. 10, which are based on a corresponding negative value of $\frac{d\alpha}{dt}$. According to Figs. 9 and 10 a decrease in the turning radius *R* with constant turning speed greatly increases the lateral reactions upon both the front and the rear axle of the vehicle. The influence of the turning speed $\frac{d\alpha}{dt}$ upon the specific lateral reactions $\frac{Y_1}{G_1}$ and $\frac{Y_2}{G_2}$ is well illustrated by the graphs shown in Fig. 11. These graphs are based upon equations (20) and (21) in which $\frac{dv}{dt}$ is taken as zero and the coefficient k as $k = 0.5$.

Referring to Fig. 11 it will be seen that a decrease in $\frac{d\alpha}{dt}$ is accompanied by a sharp decrease in the specific lateral reactions acting upon the two axles of the vehicle. A particularly sharp decrease in the reaction forces is obtained with negative values for $\frac{d\alpha}{dt}$, that is at the instant when the vehicle comes out of the curve and resumes straight line travel.

The interrelationship between the specific lateral reactions and the travelling speed *v* for different values of $\frac{dv}{dt}$ is exemplified in Fig. 12. These charts are based upon equations (20) and (21) with $\frac{d\alpha}{dt} = 0$ and $k = 0.5$. It will be noted that changes in the values of $\frac{dv}{dt}$ have but little influence upon the specific lateral reaction.

The charts given in Figs. 4-12 show the influence of the speed *v* upon the specific lateral reactions $\frac{Y_1}{G_1}$

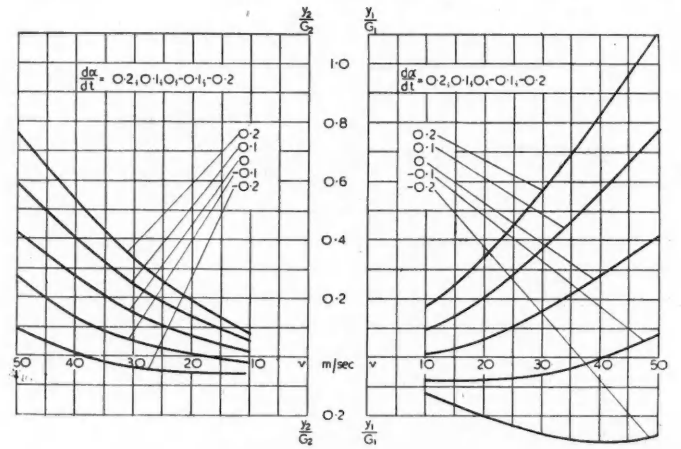

Fig. 11. **Lateral reactions *vs* speed *v* for different values of $\frac{d\alpha}{dt}$**

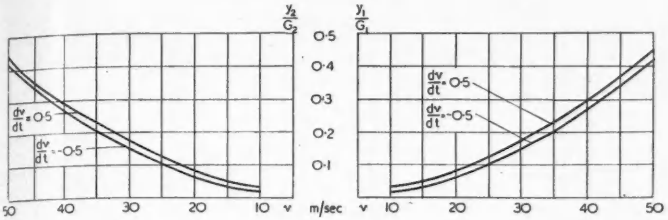

Fig. 12. **Lateral reactions *vs* speed *v* for different values of $\frac{dv}{dt}$**

and $\frac{Y_2}{G_2}$ over a wide range of conditions. In many of these cases the specific lateral reactions are considerable and in excess of the lateral stability of the vehicle, that is to say, lateral skidding of one of the axles will take place with even smaller lateral reactions so that equations (20) and (21) on which these graphs are based, cease to apply. The graphs given in Figs. 4–12 therefore cannot be considered to be in agreement with actual conditions as far as large values of $\frac{Y_1}{G_1}$ and $\frac{Y_2}{G_2}$ are concerned.

AGE HARDENING OF THE SOLID SOLUTION ALUMINIUM-ZINC.

By J. HÉRENGUEL and G. CHAUDRON. (From *Revue de Métallurgie*, Vol. 41, No. 2, February, 1944, pp. 33-41).

IT is well known that solid solutions of aluminium-zinc do not exhibit age hardening when they are prepared from industrial metals. But age hardening can be produced by adding a very small amount of magnesium to the alloy.

This investigation is concerned with a study of solid solutions of aluminium-zinc made up from metals of very high purity. It was found that in this case age hardening takes place to a very considerable degree. An examination was also made of the effects of small additions of magnesium, iron and silicon to the high-purity alloy.

The high-purity alloys were prepared from the following metals :—

Refined aluminium 99.993 per cent pure ;
Double refined magnesium ;
Zinc, 99.994 per cent pure ;

while the industrial alloys were prepared from

Aluminium, 99.5 per cent pure with 0.30 per cent Fe and 0.20 per cent Si.
Electrolytic zinc, 99.97 per cent pure.
Technical magnesium, 99.8 per cent pure without copper.

The following alloys were prepared :

(*a*) *Pure Metals.*

Binary solid solutions of aluminium-zinc of 3, 6, 5, 10, 12 and 20 per cent zinc content.

For the purpose of studying the influence of magnesium upon age hardening : Al-Zn alloys, with 6.5 per cent Zn and 0.05, 0.1, 0.3 and 0.6 per cent Mg ; also Al-Zn alloys with 12 per cent Zn and 0.02, 0.05, 0.1 and 0.3 per cent Mg.

For investigating the influence of iron upon age hardening : Al-Zn alloys with 6.5 per cent Zn and 0.1, 0.4 and 1.0 per cent Fe.

(*b*) *Industrial Metals.*

For the purpose of studying the influence of the magnesium content upon age hardening : Al-Zn alloys with 6.5 per cent Zn were prepared with magnesium additions of 0.05, 0.1, 0.2 and 0.5 per cent, these alloys also containing 0.4 per cent manganese.

The cast bars, which measured $16 \times 16 \times 100$ mm., were easily rolled into sheets upon heating to 450 deg. C. Only the 20 per cent Al-Zn alloy was rolled after heating to 400 deg. C. Water quenching of the sheets was carried out from 450 deg. C. The pure alloys containing magnesium exhibited a strong tendency to grain growth when heating was carried out in air, but not when heated in the salt bath. This must be ascribed to the more rapid heating of the metal effected by immersion.

Age hardening took place at a room temperature of 15-18 deg. C.

Unlike the solid Al-Zn solutions of industrial metals, the solid solutions of the pure metals displayed a very considerable amount of age hardening subsequent to the quench.

The increase in hardness was found to depend largely upon the zinc content of the alloy, a content of 3 per cent being quite ineffectual in this respect. But alloys with 6.5 per cent zinc and more exhibited very pronounced age hardening tendencies, as shown in Fig. 1.

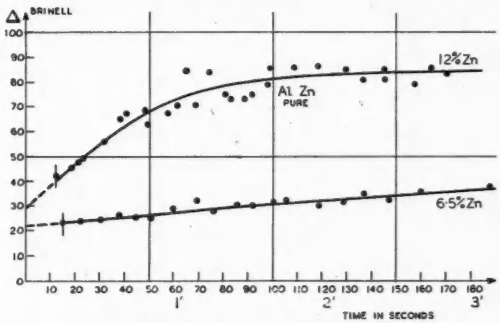

Fig. 1. **Pure Al-Zn alloys. Increase in hardness at room temperature after quenching from 450 deg. C.**

Here a particularly rapid rise in Brinell hardness is seen to take place within 10 seconds after the quench. Since it was not feasible to measure the hardness within less than 10 seconds after the quench, the actual hardness prevailing immediately after the quench could not be measured. The development of age hardening within 35 minutes after the quench is charted in Fig. 2. The latter also shows that the 3 per cent alloy displayed no age hardening at all. The length of time required for the development of maximum hardness was found to be the following :—

Al-Zn alloy with 12 per cent Zn : 15 minutes.
" " " 10 " " " : 3 hours.
" " " 6,5 " " " : 24 hours.

With 20 per cent zinc content the increase in hardness was found to take place so rapidly that accurate measurement proved impossible.

It was found that in the case of the Al-Zn alloys prepared with pure metals the increase in ultimate tensile strength after quenching was analogous with the increase in hardness. As, however, a longer time was required to execute the tensile test, it was not possible

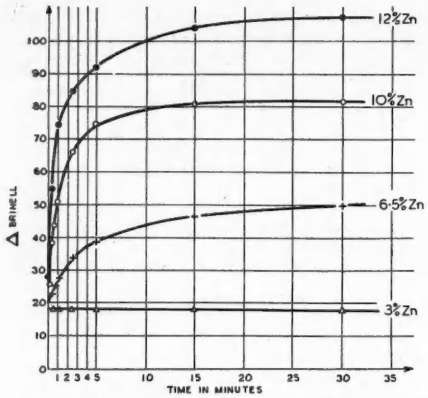

Fig. 2. **Pure Al-Zn alloys. Increase in hardness at room temperature after quenching from 450 deg. C.**

to obtain the ultimate tensile strength values prevailing within less than one minute after quenching. The test data recorded with zinc contents of 3, 6, 5, 10 and 12 per cent are plotted in Fig. 3. The increase in the elastic limit of the alloy with the time after quenching is given below :—

Time of age-hardening.	Zn = 3%	Zn = 6.5%	Zn = 10.0%	Zn = 12%
1 minute	2	5	13.4	14.5 kg./sq. mm.
2 minutes	2.2	7	14.0	14.8 ,,
15 ,,	2.1	9	14.5	17.2 ,,
15 days	2.2	10	15.7	17.2 ,,

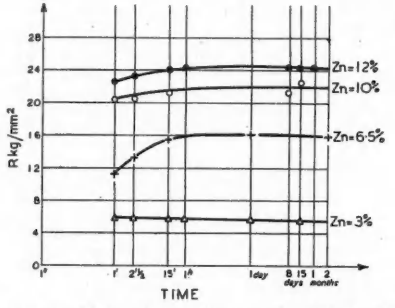

Fig. 3. **Pure Al-Zn alloys. Increase in ultimate tensile strength at room temperature after quenching from 450 deg. C.**

The influence of additions of magnesium to pure Al-Zn alloys was studied on alloys with zinc contents varying from 6.5 to 12.0 per cent. The behaviour of the 12 per cent Zn alloy is charted in Fig. 4, where it is seen that the process of age hardening after quenching is not preceded by a period of incubation if the magnesium percentage is small. In the case of the alloy containing 6.5 per cent Zn and 0.6 per cent Mg, incubation does, however, take place, and age hardening does not commence until five minutes after the quench.

The considerable difference between the age hardening characteristics of pure and commercial Al-Zn alloys can be explained by the action of iron and silicon which are normally present in commercial aluminium. In order, therefore, to study the influence of iron in this respect, different amounts of iron were added to an Al-Zn alloy with 6.5 per cent Zn prepared of pure metals. Referring to Fig. 5, it will be seen that

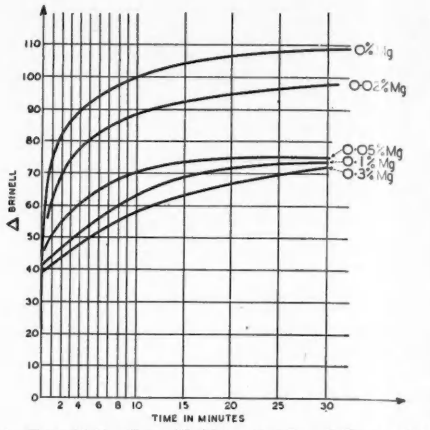

Fig. 4. **Pure Al-Zn alloy with 12 per cent Zn. Influence of Mg additions upon age-hardening at room temperature after quenching from 450 deg. C.**

the presence of Fe in the alloy exercises an important influence upon the age-hardening characteristics. Even 0.1 per cent of iron leads to a considerable decrease in the age-hardening effect. The characteristic is still further depressed with the presence of 0.4 per cent iron in the alloy ; while an increase in the iron content to 1.0 per cent causes relatively little additional change in the age hardening characteristic. This is due to the limited solubility of the iron in the aluminium. By extrapolation the speed of the age hardening process immediately after the quench can be obtained as follows

Fe %	Initial age-hardening speed	ΔT Brinell	ΔD Brinell	$\frac{\Delta D - \Delta T}{\Delta T} \times 100$
0	2.35	22	60	172
0.1	2.25	24	50	110
0.4	1 60	28	43	54
1.0	0.45	30	42	40

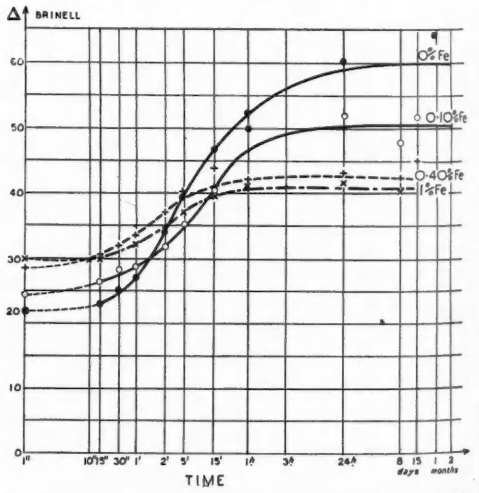

Fig. 5. **Pure Al-Zn alloy with 6.5 per cent Zn influence of Fe upon age-hardening at room temperature after quenching from 450 deg. C.**

Where A_T is hardness after quenching and A_D hardness after age hardening the action of iron is thus seen to be quite different from that of magnesium. In the case of small additions of iron the age hardening speed is but little affected; and while its retarding influence grows with rising percentages, its influence yet remains less pronounced than that of magnesium. But it is obvious that in the case of commercial Al-Zn alloys it is the iron which impedes their age hardening.

The influence of magnesium upon the age hardening process was studied on a commercially pure alloy containing 6.5 per cent zinc, 0.3 per cent iron, 0.2 per cent silicon and 0.4 per cent manganese, to which 0.05 per cent, 0.1 per cent, 0.2 per cent and 0.5 per cent magnesium respectively were added. The age hardening characteristics obtained are chartered in Fig. 6, where the small amount of age hardening in the absence of magnesium is particularly noteworthy.

The effect of magnesium is obvious, as is also the long incubation period required. The slowness of the age hardening process is particularly well illustrated in Fig. 7, where hardening speed and intensity are charted as functions of the magnesium percentage. The incipient age hardening speed is seen to be especially low if the magnesium content exceeds 0.1 per cent. Thus both magnesium and iron exert a retarding effect upon the age hardening process. The degree of final hardness is, however, increased with rising magnesium content; while it is decreased with rising iron percentage. Therefore magnesium offers a means to impart age hardening properties to commercial Zl-Zn alloys containing iron and silicon.

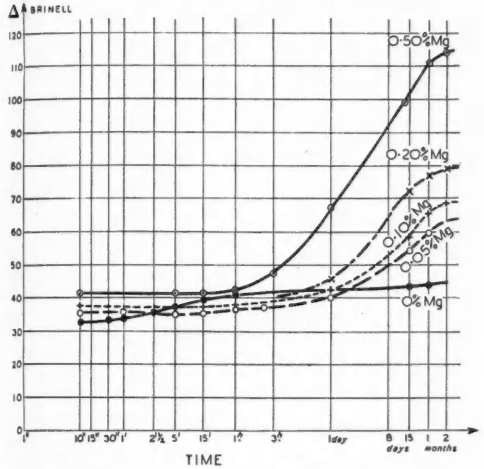

Fig. 6. **Industrial Al-Zn alloy with 6.5 per cent Zn. Influence of Mg upon age-hardening at room temperature after quenching from 450 deg. C.**

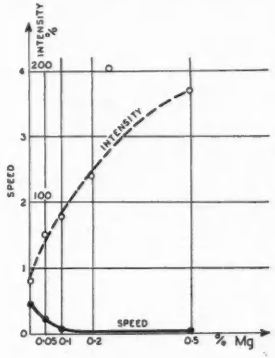

Fig. 7. **Industrial Al-Zn alloy with 6.5 per cent Zn. Initial speed and intensity of age-hardening at room temperature after quenching from 450 deg. C. or function of the Mg content.**

CARBON, A MATERIAL FOR SWITCH AND CONTROL GEAR.

By F. HOFMANN and L. WEILER. (From *Elektrotechnische Zeitschrift*, No. 13-14, April, 1943, pp. 181-184).

MODERN switchgear, despite the great strain imposed on it, must be of very high reliability and have a long life with little maintenance. The latter condition in particular depends, to a large extent, on the contact pieces of the switch which are subject to considerable wear. The life of contact pieces is, in general, a function of the switching frequency and of the intensity of the current controlled by the switch. The conditions under which switches, such as are used in industry, operate vary from one to three switching operations a day to 1000 and more operations per hour, and the current intensity may vary from a few amperes to 500 amperes and more, depending on the size of the machine controlled and the voltage used.

For this variety of conditions, contact pieces of copper have in general proved satisfactory, and the wear became considerable only in cases where the switches were used for intermittent operations with especially high switching frequencies. Special design of the contact pieces and the use of special materials, however, have made it possible to reduce the wear.

Some time ago, in the course of this development, carbon contacts were also introduced. It is true that carbon was already being used for this purpose some decades ago. But the manufacture of carbon then began to lag behind the development in the switch gear industry in general, which therefore resorted to metal contacts, using mainly copper. The manufacture of carbon has, however, reached a stage at present which makes it possible, in many cases, to return to carbon as a contact material.

1. *The Production of Carbon Contacts.*

The carbon used for contact pieces is manufactured from various prime-carbons, like coal, soot, coke, anthracite, graphite, etc. The solid usually de-gassed prime materials are pulverised in mills and, according to the use to which the finished carbon is to be put, one or more of the prime carbons is mixed with tar or pitch and thoroughly kneaded in special machines. The carbon paste is then pressed into the required shape, and the raw pieces are baked in furnaces fired with generator gas. The temperature is slowly increased to about 1300 to 1400 deg. C., so that the carbon is degassed without cracks. Baking and cooling takes two to four weeks, depending on the size of the piece. By this process the valuable qualities of the carbon, discussed below, are not only maintained, but improved; they can be still further improved, if the piece is subsequently baked at 3000 deg. C. in the electric furnace, a treatment which transforms the hitherto amorphous into crystalline carbon. The high quality carbon produced by this process has a higher temperature and arc resistance, and is therefore the material normally used for carbon contact pieces.

2. *The Suitability of Carbon as a Material for Contacts.*

The almost universal use of copper as a contact material is due to its high electrical and thermal con-

ductivity and to its relatively small contact resistance. In this respect carbon contacts are inferior. While the specific resistance for copper is 0.0174 Ω mm²/m, it is 25 Ω mm²/m for the type of carbon normally used as contact material. However, as the path of the current in the contact piece itself is very short and the cross-section relatively large, the electric losses in the carbon itself can be disregarded.

The conditions are, however, less favourable as regards the contact resistance. In the following, the resistance between a copper and a carbon contact will be considered first. This contact resistance is only 30 times the resistance between two copper contacts assuming equal contact pressure and equal current density. In the course of an experiment the voltage drop between a copper and a carbon contact was found to be 1 volt. When, subsequently, the carbon contact was replaced by a copper contact, the voltage drop was reduced to 0.03 volts. This figure will, however, increase considerably as soon as the contact faces oxydise or become chemically affected by vapours. But these thin layers are usually swept away by the impact and friction in the switching operation by which the original low contact resistance is usually restored.

Carbons being chemically inert, these variations of the contact resistance do not occur. But the heat generated at the contact is considerable, and as the heat conductivity of carbon (0.48 W/cm deg. C.) is far below that of copper (3.8 W/cm deg. C.), the dissipation of the heat constitutes a major problem.

These conditions improve, if carbon is used for both contacts, in which case the contact resistance is about one-third of the copper-carbon resistance. As the ohmic resistance of carbon decreases if the temperature increases, both the contact and conductive resistance will decrease by about 25 per cent when the switch is actually in operation. However, the use of two carbon contacts will in general be possible only in new constructions, and not for replacement in existing switches.

The properties of the carbon as described above would appear to make its usefulness as contact material doubtful. But in many cases the high contact and conductive resistances of the carbon are of no consequence, mainly where the current density is comparatively small, which means where the switch is not fully utilized, or if the density is great and the cooling adequate. In some cases a high contact temperature will be preferred to frequent maintenance work.

The advantage of a carbon contact over a metal contact is based on the physical and chemical properties of the carbon. It sublimates only at 3,900 deg. C. which prevents the welding together by the electric arc, not only of two carbon contacts, but also of one carbon and one copper contact. Compared with this, the melting point of copper is at about 1100 deg. C., and, as the arc has a higher temperature, the metal at the contact face melts and partly evaporates. When it solidifies again, both contact faces may, under certain circumstances, weld together and easily cause trouble, particularly in the case of magnetic switches.

Another clear advantage of carbon contacts is that the products of oxidation are gaseous and that carbon is chemically inert. Therefore, no films will be formed on the contact faces as a result of oxidation or other chemical reactions, as is the case of copper contacts, where these semi-conductive layers may cause trouble, particularly if the switches are only rarely operated. The frequency and scale of the disturbances due to layers on the faces of copper contacts can be reduced by means of special design of the switch, by the use of sliding or revolving contacts or by contact "greasing." But carbon possesses in itself greasing qualities and experiments have proved that on off-current switching of a moving carbon contact on a fixed copper contact, the latter had a life five times longer than when the moving carbon contact was replaced by one of copper.

Further, the arc voltage is more favourable to carbon than to copper, a quality which is of particular importance for starters and regulators.

In addition, the flow of contact material from one contact to the other is smaller in the case of carbon contacts, mainly at low densities.

The compressive strength of copper is of the order of 3000 kg./cm², and that of carbon 1000 to 1600 kg./cm², according to the type used. Nevertheless, this figure is sufficient for all practical purposes. It should be borne in mind that carbon is a ceramic, and that as such its physical properties differ widely from those of any metal and that therefore, factors pertaining to identical mechanical properties in both cases cannot be compared. Carbon used for contacts should be of high shock resistance. When replacing copper by carbon contacts it may sometimes be of advantage to use larger dimensions in order to come nearer to the mechanical strength of the metal contact. The specific gravity of carbon is about one-third of that of copper, so that the mass of the carbon will remain in general below the mass of the copper contact.

Carbon contacts have the advantage of possessing a very low modulus of elasticity (600 to 1200 kg./mm²) whilst the corresponding figure for copper is 11,000 kg./mm². This leads to the assumption that, at a given pressure, carbon makes contact at a greater number of points, each of which has a larger surface, than is the case with copper contacts. Incidentally, this explains why the contact resistance of carbon contacts is so much lower than would have been expected, considering the high ohmic resistance of the carbon only.

3. *Experimental and Operational Experience.*

(*a*) Carbon contacts in magnetic switches. Carbon has been used in magnetic switches for electric elevators (Fig. 1) since 1935. The fixed contact consists of an auxiliary part, made of arc-resisting carbon, and of the main contact piece, made of metalled carbon. The movement of the moving contact is such that contact is established first with the part made of arc-resisting carbon, and, subsequently, with the main part made of metalled carbon which has a comparatively low conductive and contact resistance. Thus the arc, and therefore the scorching of the contact material, occurs on the arc-resisting material, while the main contact is made over the metalled carbon with consequently lower

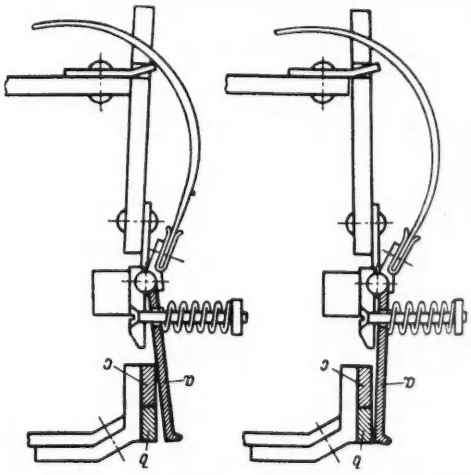

Fig. 1. **Carbon contacts in magnetic switches:** Left—position when establishing or breaking contact. Right—switch-on position.

losses and lower heat generation. Switches of this design have shown very good results, and have the additional advantage that the switching impact is less audible than that of metal contacts.

(*b*) Carbon contacts in oil-immersed controllers. As a result of extensive experiments in recent years, it has been possible in many cases to replace copper contacts in 3-phase oil-immersed controllers for intermittent operation by carbon contacts.

The rotor windings are controlled by drum-type controllers, the drum bearing copper contacts on which the carbon contact pieces slide. On the other hand, the stator windings are switched by impounding contacts, the fixed contacts being of carbon and the moving contacts of copper.

The use of carbon instead of copper for the fixed contacts results in doubling the life of the contact pieces without impairing the controller. It should be pointed out that the use of carbon does not make it necessary to purify, or change, the oil more often than if only copper contacts are used. These particularly favourable conditions are brought about by the cooling effect of the oil on the carbon contacts. This effect is incidental, as the presence of the oil is in any case necessary for the extinction of the arc and for making the switch choke-damp-proof.

These controllers, a large number of which are used in mines, show a much better performance than the types with only copper contacts which were previously used.

(*c*) Carbon contacts in other controllers (not oil-immersed). The performance of these controllers is impaired by the difficulties arising in the dissipation of heat. Experience shows that favourable conditions exist if the controller is operated at 60 to 70 per cent of its rated capacity, in which case the life of the carbon contacts equals the life of copper contacts at full load.

Only apparatus with one carbon and one copper contact have been discussed. The reason for this is that only in exceptional cases will it be possible, for purely physical and constructional reasons, to replace both copper contacts in an existing apparatus by carbon contacts.

4. *Fastening of Carbon Contacts.*

Experiments have shown that special care must be taken in fastening carbon contacts in their holders, not only for reasons of mechanical strength, but also because of the transition resistance and the heat dissipation. Experiments have been carried out with carbons fastened by the following methods :—

(*a*) Rigid connection :

- (α) carbon galvanised (with copper) and soldered to the holder. Generally not used for moving contacts.
- (β) metalled carbon welded to holder.

(*b*) Interchangeable connection :

- (α) metal nuts pressed into carbon ;
- (β) carbon held by special fitting of brass or copper ;
- (γ) metalled carbon welded to metal socket ;
- (δ) metal socket formed by spraying.

} The carbon prepared by one of these methods is fastened by screws to the carbon holder.

Of all the above methods, those of welding the carbon to metal and of spraying on a metal socket have proved the most satisfactory (see Fig. 2).

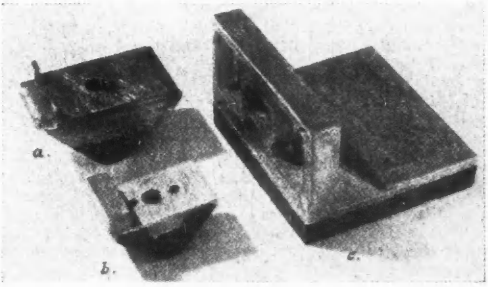

Fig. 2. **Carbon contacts.**
(a) Moving carbon contact with soldered-on socket.
(b) " " " " sprayed-on socket.
(c) Fixed " " " " "

INSTRUMENTS FOR TECHNICAL STROBOSCOPY.

By P. DREWELL, Lübeck. (From *Archiv für Technisches Messen*, July, 1942, pp. 63-66).

INSTRUMENTS WITH MECHANICALLY MOVED DIAPHRAGMS.

A stroboscope developed on the principle of moving diaphragms is shown in Fig. 1. The slit-disc (c) is driven by a motor (a), the speed of which is regulated between 600 and 3000 r.p.m. through a variable resistance forming part of the instrument. Fine speed-control is carried out by means of an eddy-current brake which consists of a permanent magnet (b) the position of which can be adjusted to the braking force applied to the disc.

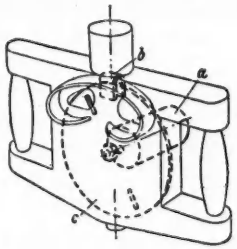

Fig. 1. **Diagrammatic view of a slit-disc stroboscope.**
(a) motor ; (b) eddy-current brake ; (c) slit disc.

The instrument is provided with seven interchangeable slit-discs, with slits numbering 1, 2, 4, 6, 10, 12 and 24 respectively, in order to ensure a wide range. The highest frequency which can be observed with this instrument is 1200 per second. With discs having 1, 2, 4 and 10 slits, observation must be monocular. In the case of 6, 12 and 24 slits the distance between the slits corresponds roughly to the mean eye spacing and observation can be binocular. The instrument is intended mainly for the measurement of rotating speeds and oscillating frequencies. For such purposes, the speed of the motor can be read from a tachometer, and the reading multiplied by the number of slits in the disc which gives the observation frequency.

For stroboscopic observation proper, the observation time (t), i.e., the duration of the observation which rules the definition of the stroboscopic picture, is plotted as a function of the observation frequency, see Fig. 2. This diagram shows also the ratio of observation time to the length of the period T, and determines the luminosity. The curve elements apply to the various slit-discs. It will be seen from the diagram, that, e.g., an object revolving at 100 r.p.m. may be observed at $t = 1, 2 \cdot 10^{-4}$ s. or at $t = 2.4 \cdot 10^{-4}$ s., the object revolving during observation through an angle of 4.3 deg. or 8.6 deg. respectively, with 1.2 per cent or 2.4 per cent of the true luminosity of the object being utilised. The

curves in Fig. 2 apply only when the fixed slit-disc, supplied with the instrument, is fitted in front of the rotating slit-disc. To allow observation from a distance, an optical prism can be fixed to the instrument which, incidentally, will ensure distortionless observation.

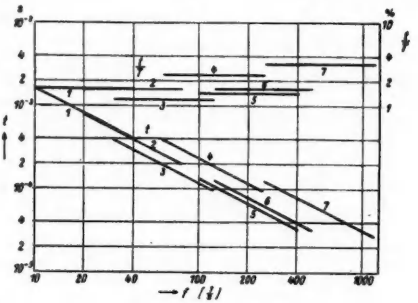

Fig. 2. **Observation time t and luminosity t/T as a function of the observation frequency f of a slit-disc stroboscope.**

A particularly handy instrument was developed in which the slit-disc is rotated by a hand crank. Coupled to the disc is a tachometer whose pointer can be stopped in any position by a small lever. The speed of the disc is increased gradually until a steady picture of the object is attained, the pointer of the tachometer is then stopped and the reading can be taken. It should be noted that the measurements derived from observation of steady stroboscopic pictures can be interpreted in various ways.

In the case of stroboscopes with revolving diaphragms —such instruments have also been produced with a clockwise drive—it is always difficult to obtain a sufficiently constant speed for prolonged observations. This disadvantage is overcome in the "Oscilloscope," according to List, by using an oscillating diaphragm in the place of a revolving one, the natural frequency of which may be adjusted by varying the length of the spring of the oscillating system. The effective spring length is indicated as a measure of the oscillation frequency. The drive is ensured by an electro-magnet controlled by the oscillation itself and fed from a dry cell.

These instruments can be used also for producing short light-flashes, the diaphragm being located in such case between the object and the source of light. For the same purpose, arrangements have been devised in which the object is not briefly illuminated in its entirety, but a strip of light is allowed to pass over the object, thus representing an inversion of a camera with focal plane shutter The easiest way to accomplish this is by means of a cylinder provided with axial slits and revolving about a linear luminous source. Another method is to deflect, periodically, a band of light by a revolving or tilting mirror. These arrangements will prove suitable for stroboscopic observation only, providing the object moves in the direction in which the ray of light travels, as otherwise it will appear more or less distorted, according to the speed of light deflection. As this requirement, however, is but rarely dulfilled, the scope of application of such instruments is limited.

GLOW LAMPS AS STROBOSCOPIC LUMINOUS SOURCE.

Notwithstanding its low intensity, the glow lamp is popular as a source of light for the purpose of stroboscopic measurement, or control of revolutions and frequencies since it is cheap and may be operated in very simple circuit arrangements. It is available in varied types and sizes and can be operated on either A.C. or D.C. The latter requires, however, special circuit arrangements. More frequently, glow lamps are operated on A.C. taken either from the mains or from a special generator, e.g., a tuning-fork buzzer. In order to make the lighting frequency equal to that of the current, one half-wave must be suppressed. Where this is not obtained automatically by the dyssymetry of the electrodes in the glow lamp, the latter can be connected to the cource via a rectifier. Another, and often simpler method, is to apply a D.C. bias to the lamp, and to choose D.C. and A.C. voltage in such a way that the lamp will only light on one of the half-waves. In order to obtain brief flashes, the A.C. tension may be distorted so as to leave a brief peak within the working range of the glow lamp. If the mains are used as the source, the distortion can be obtained, for example, by using a choke coil with an over-saturated iron core. If the glow lamp is operated from an amplifier, the required shape of the voltage curve may be obtained by suitable grid control of the valves.

It should be noted that standard glow lamps contain a series resistance which renders them unsuitable for use in special arrangements, e.g., in Hittorf's flashing circuit. For such purposes, lamps without series resistance are obtainable.

INSTRUMENTS WITH HIGH-PRESSURE LAMPS AS LUMINOUS SOURCE.

In order to allow a wide application, the flashing stroboscope must produce sharp and luminous pictures for all motion processes under consideration in industry. The definition of the stroboscopic picture depends, not only upon the duration, but also on the deviation in the timing of the flashes, since the eye will mostly perceive several of the impressions caused by the flashes as a simultaneous picture. For example, if we allow a definition latitude of 1 mm. in a motion process at 100 m. per sec., the sum of flash duration and deviation should not be greater than 10^{-5} s. Since periodic processes taking place at great velocity have generally a great motion frequency, it is necessary that flash duration and deviation decrease with increasing frequency.

The luminosity of the flashes should preferably be sufficient to allow stroboscopic investigations to be carried out in undarkened rooms.

To make the stroboscopic effect simply visible, e.g., for stroboscopic measurement of revolution and slip, a luminosity causing a contrast of only 1 per cent on the object will be sufficient. But where it is desirable to investigate objects showing by themselves only small light contrast, considerably higher luminosities will be required, the degree of which will depend upon the size of the object, its colour and the amount of general lighting. Since stroboscopic examination is limited to comparatively small parts it should be possible to concentrate the light of the stroboscopic lamp on small areas.

The frequency of the flashes should be adjustable within wide limits, in order to cope with the largest possible variety of processes. The lower limit is determined by the consideration that perfect observation at flash frequencies of less than 10 per sec. is no longer possible due to the great flicker effect. The upper limit is usually set by the luminous sources themselves. For gas discharge lamps operating in Hittorf's flashing circuit it is several 1000 cycles per second. Processes of a higher frequency can be examined in such a way that flashes are emitted only on each second or third cycle of their motion.

Exceptionally suitable stroboscopic sources of light are high pressure mercury-vapour lamps. Their luminous density is very high, especially when the discharge current is high. The electrode spacing and the luminous surface can consequently be kept small, thus allowing the light to be concentrated into a fine beam. In order to control the lamps, special grid controlled discharge valves have been developed. Fig. 3 shows

an instrument using a mercury-vapour lamp with approximately 0.25 ats gas pressure as a source of light. The lamp is fed through a grid controlled valve with filament cathode and hydrogen or helium filling. Lamp and control valve are connected in series in the discharge circuit of a condenser. The valve controlling the timing, duration and intensity of the discharge is controlled in turn by a tuned circuit designed carefully with a view to securing a very constant frequency. In addition, there is a frequency measuring circuit which indicates, by means of a moving-coil instrument the set-flashing frequency with a maximum error of 2 per cent, which can be reduced in special cases to 0.3 per cent. The instrument, which is operated on the A.C. mains has no moving parts.

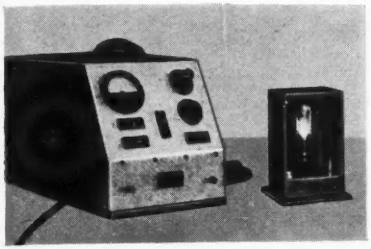

Fig. 3. **Flashing stroboscope.**

The frequency can be set within a range of 6 to 200 cycles per second in one model, and in another between 12 and 800 cycles in four stages, and can be finely regulated within each stage by means of a variable resistance. In order to synchronize the flashes with the process under investigation an A.C., or pulsating D.C. potential can be applied to the circuit. The energy required for synchronising is very small, since a voltage of only 0.5 V. is sufficient and as the imput resistance for this potential is 5000 ohms. By using a synchronising potential of several volts, the flashing frequency can be carried over an octave without making any adjustment to the instrument, so that objects with greatly fluctuating motion frequency can be brought to an apparent standstill.

To obtain higher flashing frequencies, the capacity of the condenser must be reduced and the duration of the flashes will decrease correspondingly. The luminosity is sufficient for all visual observations. Once the instrument is synchronised, sharp and well lighted photographs of the object can be taken by overloading the lamp for the exposure. A button is provided for this purpose, but in order to take silhouettes, individual flashes will be sufficient.

The instrument can also be built with two lamps connected in series and may be used where better lighting is required for observation, but the main advantage of this method is that it permits checking whether two motion processes are in phase. Another special model was built for a frequency range of between 25 and 3000 flashes per sec.

For observations on large objects and for taking a sequence of stroboscopic pictures, a high capacity instrument has been developed which uses a high pressure mercury-vapour lamp of about 6 ats pressure as the source of light. In this case the lamp is controlled by a discharge tube with a filament cathode which, despite the discharge peaks reaching 3000 amps. has a satisfactorily long life. The frequency of this instrument can be varied between 5 and 100 cycles per sec., and in addition, it is possible to give individual flashes or a short series of flashes. For remote control of the main circuit a special instrument is provided; this is connected by cable with the main instrument.

This controlling instrument, which also contains a frequency measuring circuit and connecting bushes for synchronising, may be used alternatively as a separate unit for operating a mercuty-vapour lamp of 0.25 ats pressure within a frequency range of 30 and 1000 cycles.

The lamp in the main instrument and its oven which raises it to the necessary operating temperature of about 500 deg. C., is incorporated in a reflector, in front of which can be placed a double optical-condenser. As the light emitting surface of the lamp is only 0.5 sq. cm., it is possible to obtain an exceptionally fine beam of light. The luminous intensity which at the peak of the flash exceeds 1,000,000 CP makes the instrument not only suitable for observing and recording large objects, but more particularly for serial records of single motion processes on a stationary plate or on a steadily progressing film. Due to the short duration of the flashes which lies between 2 and 0.8×10^{-5} secs., depending on the frequency, very sharply defined pictures are obtained by this application of the instrument as a "time extender." The possibility of producing short series of flashes with very accurate time limits is often of advantage, especially as these flash series can be controlled by the actual process to be recorded. Where the instrument for such records is controlled by a potential of known and constant frequency, both the type of process and its progress can be accurately determined.

Experiments are in progress to use lamps with inert-gas filling, both for the standard instrument as well as for the large stroboscope. Apart from the advantage that these lamps need neither be heated up, nor operated in a stove, the light flashes produced are shorter and of higher intensity. With the same expenditure of circuit gear, approximately 8 to 10 times greater luminous intensities can be obtained than with mercury-vapour lamps.

AUXILIARY INSTRUMENTS.

The most important of the auxiliary instruments used for stroboscopic measurements are those for synchronising the flashing frequency with the object frequency. The electric impulses produced by these instruments should show a steep rise so that the variations in phase position of the flashes, which occur when the object frequency varies, should remain as small as possible. The simplest conditions prevail where the object is in synchronism with an A.C. voltage, since the latter may be applied to the stroboscope either directly or after suitable distortion. When observing machine parts connected with a revolving shaft, an electromagnetic impuls machine may be used which is held against the shaft end like a hand tachometer. By turning its casing, any desired phase position of the flashes can be obtained. Where the phase-positions of definite processes are to be determined, such an impulse transmitter may be firmly attached to the machine, and the movable casing connected with a pointer moving over a stationary scale. Or else devices can be used where a contact is controlled by the object itself. If the impulse machine is fitted with a gear of a ratio, say, 100 : 99, the phase position of the impulses relative to the object will change steadily and the object will appear in a highly retarded motion.

When examining objects whose energy of motion is so small that no mechanical coupling with an impulse transmitter is possible, the required electric impulses can be produced by electromagnetic, electro-acoustic or photo-electric means. Thus, when examining the spinning process on a ring spinning-frame the steel traveller was itself used for varying the flux in a magnetic circuit and the electric impulses thus induced in a coil were applied through an amplifier to the stroboscope. An example of electro-acoustic synchronisation is the stroboscopic examination of the larynx, where the "patient" sings into a microphone, thereby synchronising the stroboscope through an

amplifier. The same method may be applied when examining musical instruments. By changing the distance of the microphone from the source of sound the phase position of the flashes may easily be modified. Photoelectric production of synchronising impulses can be carried out almost invariably where the centre round which the object revolves is fixed. In such cases the object itself can be used either to reflect, or to cut a beam of light periodically.

In the course of stroboscopic examinations it may sometimes be required to photograph the object in a certain phase position, without there being any possibility of bringing about adequately rigid synchronisation by simple means. For such cases where standard flashing stroboscopes will not be adequate, a handy instrument for producing individual flashes was developed by J. Vastmann. The source of light used in this instrument is a spark gap, the impulses being very accurately controlled by a small gas-discharge valve. The instrument may be operated in conjunction with the flashing stroboscope in such a way that the spark will be released simultaneously with the flash of the stroboscope, and the object will thus be lighted once very brilliantly in the phase position set on the stroboscope. A further special feature of the instrument is that the duration of the spark light only amounts to 2×10^{-6} secs. and sharply defined images will thus be obtained even against very rapidly moving objects. Fig. 4 shows such an instrument. It is fitted with a special release switch connected to the instrument by a cable. If the button of this switch is pushed the shutter of the camera is opened, and following this the sparking circuit is connected to the stroboscope. The latter then releases the spark automatically.

The individual flasher may also be used by itself for recording periodical and non-periodical processes. In both cases control may be by hand or by an impuls released by the object under examination.

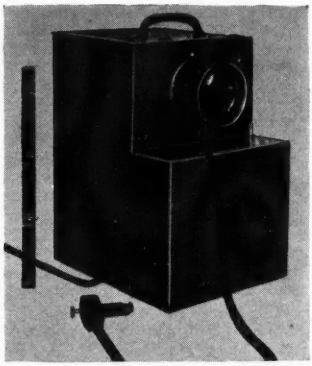

Fig. 4. Instrument for individual flashes.

CATHODE-RAY TUBE AS STROBOSCOPIC SOURCE OF LIGHT.

The upper frequency limit of a stroboscope operating with controlled discharge lamps lies at about 5000 cycles per sec. For examining processes of higher frquencies cathode-ray tubes can be used. The luminous density of a fluorescent layer is determined by the number and speed of impinging electrons, but due to the energy of the electrons being partly converted into heat on the layer, it cannot be raised indefinitely without scorching the screen. But as stroboscopic high frequency measurements are in general carried out merely to determine the frequency, the obtainable luminous intensity will be sufficient in most cases. Very little energy is required to control a cathode ray tube through its electrodes. The source of potential of adjustable frequency may be, for instance, a heterodyne oscillator, the potential curve of which can be distorted in order to shorten the flashes.

THE BRITTLENESS OF THE ENAMEL OF COATED ALUMINIUM WIRE AT NORMAL AND HIGHER TEMPERATURES.

By E. GREULICH. (From *Elektrotechnische Zeitschrift*, No. 17/18, 6th May, 1943, pp. 241-242).

THE main difficulties in the production of enamel-coated aluminum wire are due to the property of the coating to become brittle if the wire is stored for any length of time. The adhesion between the enamel and the metal core decreases and the wire becomes unsuitable for further use.

The brittling of the enamel is believed to be caused by oxidation, which is favoured by the existance of a thin layer of oxide on the metal. Experiments have been carried out with specially prepared cores and slight improvements were observed. But the cost of these methods was too high to allow them to be used commercially.

On the other hand, if the above assumption, that the brittling of the enamel is due to the absorption of oxygen, was correct, it was to be expected that the quality of the wire could be improved by using coatings of oil-less artificial resins instead of the oil-containing enamel used hitherto. The oil-less artificial resins were supposed not to absorb oxygen, and therefore not to deteriorate when stored. The validity of these assumptions, and the properties of wire with coatings of artificial resins were investigated in a series of tests. These tests were carried out with aluminium wires of 0,9 to 1.1 mm. diameter produced from one and the same batch. The coating of the wires consisted of an enamel with 37 per cent oil content in one case, and of an oil-less artificial resin in another case. A third sample had a coating of three inner layers of oil-less artificial resin and of three outer layers of the oil containing enamel.

METHOD OF INVESTIGATION.

When using aged enamelled wire, difficulties arise mainly in winding coils, as the enamel layer is apt to crack off. The winding test can, therefore, provide a suitable measure of the brittling and ageing of the enamel coating. The test must, however, be modified as the smallest mandrel diameter at which the coating still does not crack is not merely a function of the quality of the coating, but also of the diameter of the wire. It follows that, if the properties of the coating itself are to be investigated, a measure must be found which is independent of the diameter of the wire. This measure is, most conveniently, the stretching of the outermost fibres of the coating when the wire is bent.

Fig. 1 shows a mandrel of a diameter D around which a wire (diameter d) is wound. The inner fibres of the coating are upset while the outer fibres are stretched. The fibres corresponding to a diameter $D + d$ are neutral. The elongation e_w of the outer fibres is equal to the difference between the diameters of the outer and the neutral fibres, and consequently equal to the diameter of the wire:

$$e_w = (D + 2d\, e_w - (D + d) = d \qquad .. \quad (1)$$

The elongation e_w which in one turn is proportional to d is spread out evenly over the length of the wire, which is a function of the diameter of the mandrel D as well as of the diameter of the wire d; it also equals the length of the neutral fibre. The stretching *Dw* is, therefore, determined by the ratio of the elongation which is

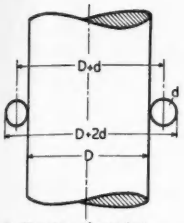

D=diameter of mandrel.
d=diameter of wire.

Fig 1.
Arrangement for the stretch test.

proportional to d and the length of the neutral fibre which is proportional to D + d:

$$\sigma_w = \frac{d}{D+d} \cdot 100 \text{ [per cent]} \quad .. \quad .. \quad (2)$$

This equation allows to calculate the stretching of the outer layer of any wire wound around any mandrel

The testing of the coatings comprise a series of individual tests, the first group of which was carried out two days after the wire had left the manufacturing process. The subsequent groups of tests were carried out at two-day intervals. The winding tests were made on finely graded mandrels, and the diameter at which the first cracks appeared were recorded. The next larger diameter was taken to indicate the stretch limit.

To investigate the influence of the temperature, the wires were stored at temperatures of 100, 120, 135 and 150 deg. C. for periods varying from ½ hour to three months. The corresponding tests were made after the samples had cooled down.

Properties when stores at room temperature (normal ageing).

(*a*) *Wires with coating of oilContaining enamel.*—The results of stretch tests on wires stored at room temperature are shown in Fig. 2. It will be seen that the ageing of oil-containing enamel begins already after 12 days. After one month the stretching of the coating has decreased to only 10 per cent, and after 100 days to 3.5 per cent. The latter figure corresponds to a minimum mandrel diameter of as much as 28 times the diameter of the wire.

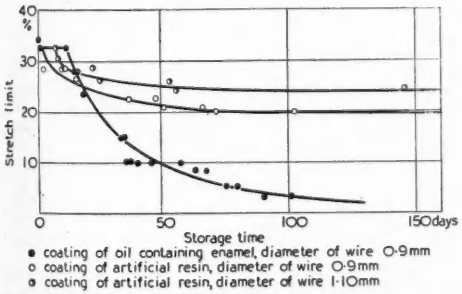

Fig. 2. **Stretch limit of coatings of wires stored at room temperature.**

(*b*) *Wires with artificial-resin coating.*—On the other hand, wires with an artificial-resin coating have, after 150 days, still a stretching limit of 10 to 24 per cent. which corresponds to a mandrel diameter of only four times the diameter of the wire. It seems therefore that wire with artificial resin coating can be stored indefinitely.

(*c*) *Wires with combined coating.*—The behaviour of wire with a combined coating is somewhere between the behaviour of wire coated with coil-containing enamel and of wire with artificial-resin coating. During the first 14 days the stretch limit decreases from 45 per cent to 25 per cent, and remains at this value until about the 80th day. Then, within two days it drops to 10.8 per cent and decreases still further after the 110th day. The diagram in Fig. 3 has a certain similarity with the diagram for oil-containing enamel (Fig. 2) which likewise shows sudden changes, though to a much lesser degree. As the stretch limit of 23 per cent is maintained for only 80 days, the manufacture of wires with a combined coating would serve no practical purpose.

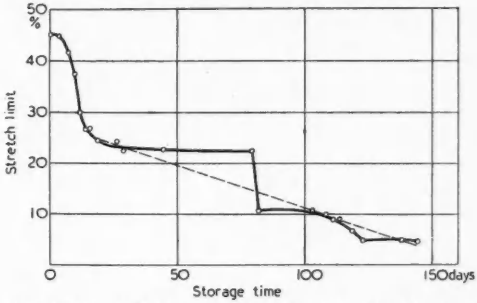

Fig. 3. **Stretch limit of a combined coating of a wire stored at room temperature.**

The influence of temperatures up to 150 deg. C.

(*a*) *Wires with coating of oil-containing enamel.*—If stored at a permanent temperature of 100 deg. C., the stretch limit of the coating of this wire rapidly decreases and reaches the very low value of 9 per cent after 56 days (Fig. 4). At temperatures of 120 to 135 deg. C. the coating becomes so brittle already after 10 days that it is practically unusable. The same happens after only four to five days if the temperature is 150 deg. C.

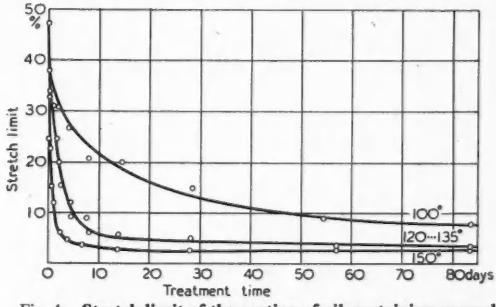

Fig. 4. **Stretch limit of the coating of oil-containing enamel of an Al-wire of 0.9 mm. diameter stored at temperatures between 100 and 150 deg. C.**

(*b*) *Wires with artificial-resin coating.*—The behaviour at higher temperatures of this coating is much more favourable (Fig. 5). Temperatures up to 120 deg. C. are entirely without influence to the stretch limit which remains within the values for wires aged at room

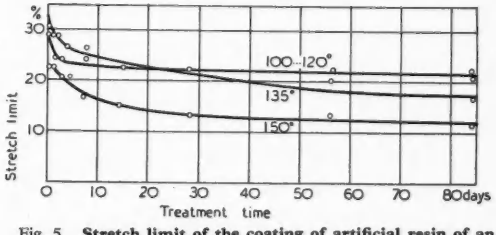

Fig. 5. **Stretch limit of the coating of artificial resin of an Al-wire of 0.9 mm. diameter stored at temperatures between 100 and 150 deg. C.**

temperature. At 135 deg. C. it is only after 50 to 60 days that it falls slightly below the value for normally aged wires though it remains still high enough for any practical purpose. A higher degree of brittleness results only when the wire is aged at a permanent temperature of 150 deg. C. In this case the stretch limit drops in 14 days to 15 per cent which is about the lowest permissible figure for practical purposes. This incidentally, means that the resin coating can be subject to occasional temperatures of up to 150 deg. C. without detriment to the quality of the wire.

(*c*) *Wires with combined coating.*—If subject to higher temperatures this coating shows even worse properties than the coating of oil-containing enamel, and at as low a temperature as 100 deg. C. the coating becomes brittle in a comparatively very short time (Fig. 6). Therefore, it would serve no practical purpose to manufacture wire with combined coating, even if its properties at normal room temperatures were favourable.

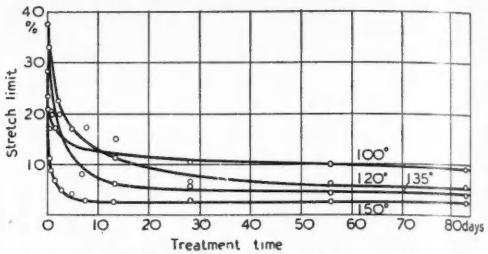

Fig. 6. **Stretch limit of the combined coating of an Al-wire of 0.9 mm. diameter stored at temperatures between 100 and 150 degree C.**

MEASUREMENT OF SMALL MOTIONS.

By K. STAIGER. (From *Archiv für Technisches Messen*, June, 1942, pp. 51/52).

THE term " measurement of small motions," as used in this article, means the measurement of the size and recording the shape, of periodic and non-periodic motions of solid bodies. These complex motions may contain harmonics of all frequencies down to zero.

For choosing the method of measurement and for assessing its situability, three conditions are of particular importance :—

(*a*) The magnitude of the deflection which determines the amplification necessary to permit sufficiently accurate readings to be taken on the instrument

(*b*) The maximum acceleration to be expected, which determines the frequency range of the instrument

(*c*) The possible distortion of the motion under investigation caused by the instrument itself.

As this article is restricted to very small motions, the majority of cases dealt with are one-dimensional. Short reference will, however, be made to the measurement of two- and three-dimensional motions.

Measurements can, in general, be carried out with or without intermediate amplification by optical, electro-optical or thermo-electrical means. The indirect methods require the use of a " transformer," for which purpose the usual inductive or capacity bridge, or differential circuits can be used. The instruments used can be classed into two main groups, according to their frequency range. In the instruments of the first group, the motion is either directly indicated, or recorded by an ink recorder. They are thus suitable only for motions which are slow compared with the setting speed of the instrument. In the second group, oscillographs are used for recording, and amplification is carried out by means of electronic valve amplifiers with no inertia. There is no upper frequency limit for this group, unless such a limit is set by the type of the mechanical-electric " transformer " and its applicability.

The first group is used mainly for control devices on machine tools, and for limit guages with automatic sifting as used in mass-production methods. The second group is used on oscillatory motions such as vibrations of foundations, vibrations due to sound, as well as on movements of machine parts (e.g., the movement of valves, jet needles in diesel engines, elongations and wobbling effects).

DIRECT MEASUREMENT.

Practically, the only method by which motions of small amplitudes can be recorded is the " scratch method." In this method a diamond sliding on a moving glass plate or a rotating glass cylinder records the movement. The thickness of the scratch thus produced is 3 to 4 μm (1 μm = 10^{-6} m). The reading error is 1 to 2 μm, which makes it possible to record deviations of only several μm with a fair prospect of success, without using levers to amplify the motion. The diamond must be applied at a pressure of about 10 grams which produces a friction of 2 to 3 grams. This is the smallest possible reaction, and applies only in case the diamond is rigidly and directly connected to the body under investigation. In practice, however, this will seldom be the case, and it will often be necessary to move the instrument, or a pointer, over the investigated part. This will require special spring and lever arrangements, and the natural frequencies of these devices will therefore have to be taken into account. The upper frequency limit of such instruments is of the order of several hundred cycles per second.

The " scratch method " is independent of any ancillary equipment, and is extensively used for measurements on aircraft, in particular of elongations and deflections, and of torsian vibrations. The relatively large mass of the parts under investigation allows the reaction of the instrument on the moving part to be neglected. A disadvantage of this system is that the evaluations of the measurements have to be carried out either under the microscope or in projection.

INDIRECT MEASUREMENT.

(*a*) *Optical amplification.* Small turning or twisting motions can be amplified simply by means of a concave mirror and a beam of light, and can be recorded photographically. This method is very sensitive to outside vibrations and requires considerable space for the beam. It is used for indicating static torsions and also, in optical pressure gauges. In the latter, the movement of a diaphragm or of a piston is transferred to a swing mirror. To reduce the effects of vibration, mirror, projection gear and recording gear can be mounted together in a rigid casing. The natural frequencies of such indicators may reach up to 30,000 cycles.

A kind of optical lever is obtained through the arrangement shown in Fig. 1, which is similar to that used by Föttinger for measuring torsion vibrations. The bevelled edge of screen S_2 moves in front of slit S1 of the fixed screen S_1, behind which the source of light is placed. Recording is made by photograph. The amplification factor is limited by the sharpness of the curve and may reach about 10.

The methods for direct optical measurement have the advantage of being simple and of influencing the movement under investigation to a relatively small degree. Their disadvantage is that the motion transmitting gear on the one hand, and the recording gear on the other, cannot be installed independently of each

other and, that there must be no object in the space between them. This limitation can be avoided if "transformers" are used which change the mechanical deviation into variations of an electric current either directly, or in two to three intermediate stages.

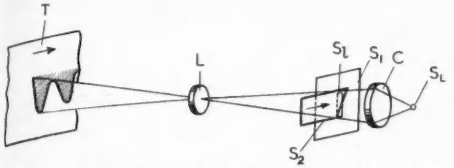

Fig. 1. **Bevelled screen method of optical amplification of motions.**

SL/L/	Source of light.
C/K/	Optical condenser.
S_1/B_1	Fixed screen.
S_2/B_2	Moving screen.
L/O/	Lens.
F/S/	Film.

(*b*) *Optical-electric transformers.* The recording or reading instrument can be separated from the motion transmitting gear, e.g., by using a photocell, as is done in Lehr's extensiometer. In this the motion is amplified by a lever which controls a slit through which a beam is directed on to a photocell. This produces a variation in the intensity of the electric current in the circuit of the cell which can be read on an indicating instrument installed separately. The amplification factor of this instrument reaches 0.5×10^5, but, owing to the large leverage employed, the instrument cannot be used for higher frequencies.

Reaction of the measuring gear can be entirely avoided if the moving part under investigation is itself used as a variable screen for a beam of light.

To avoid error in measurements involving the use of a photocell, it is necessary to keep the intensity of the source of light very constant, unless, of course, a second photocell is used at the same time and a differential measurement is taken.

Instead of simple screening, a turning mirror and two fixed screens, each with a number of alternatively transparent and opaque stripes of about 0.5 mm. individual width, are often used. One screen is placed between the source of light and the mirror, whilst the second is placed between the mirror and the photocell. The screens must be so arranged that the stripes of the first screen, when reflected from the mirror to the second screen, are parallel with the latter's stripes. Thus, even the smallest deflection of the mirror will cause a considerable variation in the light-flux reaching the photocell. This method is a combination of the slit method similar to that shown in Fig. 1 on the one hand, with the moving mirror and the photocell methods on the other hand.

Optical-electric methods are used mainly for limit gauges on machine tools; for continuous checking of bore holes; thickness of wires, etc., and ogten in conjunction with automatic compensating devices and recording instruments. The limit gauges have a range of 25 to 100 μm and an accuracy of $\pm$ 1 to 2 μm.

(*c*) *Thermo-electric transformers.* The thermo-electric transformers or Bolometers measure the change of the resistance of a heated wire whose cooling is controlled by the mechanical motion under investigation. This is done by a light vane which is controlled by the moving part and which partly covers a slit through which the cooling air passes... The air draught is produced by a magnetic field. This method is used mainly for controlling large indicating or recording instruments through sensitive measuring instruments. In such cases, the pointer of the measuring instrument serves as a vane to control the amount of cooling air passing over the heated wire of the Bolometer. The Bolometer can, however, be used also as a direct mechanical-electric transformer, where the motion is made to influence the resistance directly. This method is used in the "Mikrotaster" produced by Siemens and Halske, the accuracy at a range of 150 μm, is $\pm$ 1 μm.

The thermal inertia of the Bolometer does not impair its use in conjunction with pointer instruments, as the setting speed is of the same order for both. The sensitivity of this method can be increased considerably, and, if used in this way, the simple Bolometer gives a better performance than a large valve amplifier.

(*d*) *Inductive transmitters.* Another method uses inductive transmitters and is based on the principle of a moving piece of magnetic material in the air gap of a differential choke coil. The change of induction is measured by a bridge which, in the simplest case, is fed from the mains. To avoid errors, the supply voltage is kept constant by magnetic voltage regulators. Accuracy and zero-point deviation are of the same order as for the Bolometric or optical-electric methods. If supplied from the mains, this instrument is used mainly in connection with machine tools and as a limit gauge in mass-production. The inductive instrument is simpler mechanically than the Bolometer.

METHODS FOR MEASURING HIGH SPEED MOTIONS.

Whilst the methods described are sufficient for use in conjunction with ink recording instruments or control machinery whose motions are "slow," they are not adequate for measuring and recording high-speed motions. These require the use of valve amplifiers and oscillographs. Optical-electric instruments can, however, be used, in connection with electronic photocells. In instruments using inductive transmitters, the carrier frequency must be increased to at least four times the highest motion frequency to be measured. Up to a carrier frequency of several thousand cycles, iron-clad transmitters of a very small size can be used, e.g., as the dynamic extensiometer of the "Deutsche Versuchsanstalt für Luftfahrt [DVL]" in connection with a torsiometer of Siemens and Halske. If the carrier frequency is further increased, very light coreless coils can be used.

(*a*) *The differential-induction method.* An instrument developed by the "Forschungsinstitut für Kraftfahrwesen und Fahrzeugmotoren," at Stuttgart, for instance, uses a carrier frequency of 1 mega-cycle. In this instrument, the differential inductance of two coils is measured. The oscillator O in Fig. 2 feeds into a cylindrical air coil consisting of two symmetrical parts wound in opposition. The field of this double coil has a turning point in the neighbourhood of which its intensity increases in either direction as a linear function of the distance from the turning point (Fig. 3). Inside this coil is a smaller coil in which a high-frequency potential is induced, the amplitude being a function of its position inside the larger coil. The induced high-frequency potential, after rectification in valve R (Fig. 2),

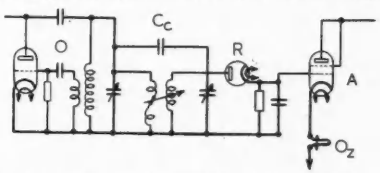

Fig. 2. **Circuit for the differential-induction method, system of the "Forschungsinstitut fur Kraftfahrwesen und Fahrzeug-motoren, Stuttgart."**

O/S/	Oscillator.
R/G/	Rectifier.
A/R/	Amplifier valve.
O_z/O_z	Loop of oscillograph.
Cc/Ck/	Condenser for additional capacity coupling.

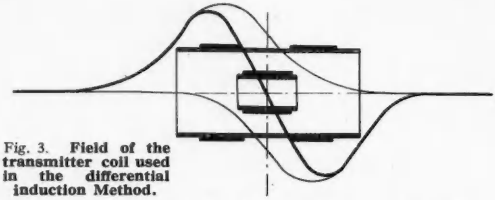

Fig. 3. **Field of the transmitter coil used in the differential induction Method.**

controls amplifier A which is connected to the oscillograph or to an indicating instrument. The additional coupling over condenser C ensures that deviations of the coil, in different directions from its neutral position, being about a reversal in the direction of the current flowing in the indicating or recording instrument. This is brought about by the potential induced in the coil now being superimposed on a high frequency potential through Cc. It thus becomes a modulation of the latter potential which acts as a carrier frequency. This means that the motions of the coil have been transformed into modulations of a high frequency which are dealt with by a rectifier and amplifier as indicated above. Merely by varying the damping of the receiver circuit and without changing the coil, the range of the instrument can be changed in the ratio 1 : 30. Zero-deviations remain very small (about $\pm$ 2 per cent of the final reading), as an electronic amplifier only is used. The general susceptibility to interferences from outside is small, as the output on the transmitter reaches up to 10^{-2} W, which is less than is reached, e.g., on the DVL extensiometer. Up to the present this method has been used for measuring deviations ranging from 10 um to 4 cm. For measurements in the samll range, the weight of the moving coil is less than 0.5 grams. The fastening of the leads causes no difficulties, even if considerable shock accelerations occur.

If the mass of the part under investigation is large enough, the coil can be controlled through a lever pressed by a spring on to the moving part. The contact pressure must, however, be large enough to ensure that constant contact is maintained between the lever and the part, even at the highest accelerations that may occur. If a lever is used, the instrument can be easily calibrated by moving the lever by a micrometer adjustment and comparing both readings.

(*b*) *The capacity method.* The transmitter of this method consists of a small condenser, formed either by the part under investigation and a plate, or by two plates one of which is mobile and controlled by the moving part. The capacity of the condenser is a reverse function of the distance between the two plates ; to maintain this function sufficiently linear, the initial distance between the plates must not be below a certain minimum.

The measuring condenser is used to influence either the natural frequency of a tuned circuit, whose potential is measured through a rectifier, or to influence, through the tuning circuit of a valve oscillator, the output of the latter and thus the D.C. component of the plate current of the oscillator valve. This arrangement is very simple and requires only one valve. With a total capacity of the tuning circuit = 150 pF, capacity variations down to about 10^{-2} pF can still be measured.

Certain difficulties exist in arranging and fastening the leads ; these must be short in order to keep the total capacity of the circuit low and their capacity must remain constant. Vibrations make the fulfilment of the latter condition usually difficult. Another disadvantage is that the capacity method, being based on the resonance of a circuit, is very susceptible to fluctuations of temperature.

The capacity method is used mainly where the transmitter must be very light; where the moving part cannot be mechanically connected to the transmitter, and where the transmitter must in no way influence the motion.

MEASUREMENT OF MULTIDIMENSIONAL MOTIONS.

In principle, two-or-three-dimensional motions can be measured by splitting them up into two or three right-angled components. If the motion proceeds in a plane, the two components can be put together immediately by applying the measurement impulses to two pairs of control electrodes of a cathode-ray tube. This method is very common in electrical engineering for measuring hysteresis loops or the charts of electron valves. Instead of cathode-ray tubes, " co-ordinate recorders " may be used.

It is more difficult to register a three-dimensional motion, as each of the three transmitters must be sensitive only to one component of the motion. The simplest way is to use an optical method.

Fig. 4 shows how a three-dimensional motion, in this case the motion of a vehicle frame can be reproduced graphically by putting together the recordings of its component motions. The graphs in Fig. 4 were recorded by the differential-induction method.

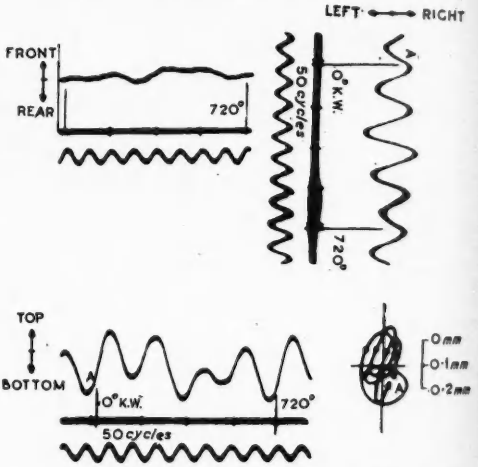

Fig. 4. **Reproduction of a three-dimensional motion from its component one-dimensional motion.**

THE ACCURACY OF THE VARIOUS METHODS.

If a deflection method is used, the accuracy is limited by the ink recording instrument which in one range must record the complete motion. Ink recorders usually have an accuracy of $\pm$ 1 per cent of the maximum deflection owing to unavoidable friction and play. If oscillographs are used for recording, the accuracy depends on the cross-section of the beam. Additional errors of the order of $\pm$ 2 to 3 per cent occur where an amplifier is used, due to distortions in the amplifier valve. The above figures refer only to deviations from the actual value, which may occur with a calibrated instrument while being used.

The absolute accuracy, on the other hand, depends on the accuracy of the transmitter and of the instrument used for calibration.

If slow motions, or only parts of motions are under investigation, the accuracy of the measurement can be increased by using zero-methods, i.e., bridge and differential methods with automatic compensation. In such cases the results of the measurements are not directly influenced by the properties of the electrical instruments used, and enables the errors to be kept considerably below $\pm$ 1 per cent without difficulty.